Journal of Zhejiang University-SCIENCE A (Applied Physics & Engineering) 2024 25(10):854-876
www.jzus.zju.edu.cn; www.springer.com/journal/11582
E-mail: jzus_a@zju.edu.cn

Review

https://doi.org/10.1631/jzus.A2400397

Check for updates

Near-term applications of superconducting digital quantum simulation

Yunyan YAO[1,2]✉, Zhen WANG[1,2]✉

[1]*Zhejiang Key Laboratory of Micro-Nano Quantum Chips and Quantum Control, School of Physics, Zhejiang University, Hangzhou 310027, China*
[2]*ZJU-Hangzhou Global Scientific and Technological Innovation Center, Zhejiang University, Hangzhou 311200, China*

Abstract: Quantum simulation, as a practical application of noisy quantum computing, has aided the study of exotic quantum matters and the implementation of algorithms that outperform classical approaches. Superconducting qubits, one of the most promising candidates for realizing universal quantum computing, possess state-of-the-art features like easy integration of qubits, long coherence time, and high-fidelity single- and two-qubit gates. These characteristics have enabled applications of digital quantum simulation in the fields of physics, chemistry, and computer science. In this review, we first present the basic concepts of superconducting qubits, quantum gates, and digital quantum simulations. We also explore recent progress in digital quantum simulations using superconducting qubits, especially in relation to quantum chemistry, quantum matters, combinatorial optimization, and quantum machine learning. Finally, we address the current challenges of digital quantum simulation with superconducting qubits, and provide a perspective on the future of the field.

Key words: Superconducting quantum circuits; Digital quantum simulation; Quantum chemistry; Quantum matters

1 Introduction

Quantum simulation (Georgescu et al., 2014) is a promising method for tackling scientific and engineering problems that cannot be effectively solved even by the most powerful supercomputers (Preskill, 2012; Neill et al., 2018; Arute et al., 2019; Zhong et al., 2020; Wu et al., 2021). Some of these challenging problems include understanding the nonequilibrium features of quantum many-body systems (Eisert et al., 2015), addressing the black hole information problem in cosmology (Bauer et al., 2023), and calculating the reaction rates of chemical and pharmacological molecules (McArdle et al., 2020). The potential advantages of quantum simulation over classical computing have been demonstrated preliminarily in random circuit sampling problems of quantum systems containing 50–60 particles (Arute et al., 2019; Wu et al., 2021), as well as in solving for the time evolution of the 2D transverse-field Ising model (Kim et al., 2023). With the rapid development of experimental platforms (Zhu QL et al., 2022; Deng et al., 2023; Bluvstein et al., 2024; Guo SA et al., 2024), the next goal for quantum simulation is to demonstrate its advantage on problems with practical relevance (Daley et al., 2022). In this way, it may have a revolutionary impact on fundamental research, applied science, and technology.

While there are no specific guidelines for implementing quantum simulation, a common approach involves using quantum two-level systems known as qubits (Nakamura et al., 1999; Martinis et al., 2002; Blais et al., 2004; Clarke and Wilhelm, 2008); these qubits serve as the fundamental units for realizing quantum computing. To form a qubit, several basic criteria must be met (DiVincenzo, 2000). It should be able to exist in well-characterized $|0\rangle$ and $|1\rangle$ states, allow unitary operations to be performed between $|0\rangle$ and $|1\rangle$, enable the determination of the qubit's state, and most importantly, have a long coherence time (or the lifetime of the qubit). Since Feynman proposed the concept of quantum simulation in 1982 (Feynman, 1982),

✉ Zhen WANG, 2010wangzhen@zju.edu.cn
Yunyan YAO, cooper_yao@zju.edu.cn
Yunyan YAO, https://orcid.org/0000-0002-2503-670X

Received Aug. 8, 2024; Revision accepted Sept. 13, 2024; Crosschecked Sept. 25, 2024

a variety of experimental platforms have been developed, including the nitrogen-vacancy center (Weber et al., 2010), cold atoms (Greiner et al., 2002; Browaeys and Lahaye, 2020), trapped ions (Blatt and Roos, 2012), superconducting circuits (Nakamura et al., 1999; Martinis et al., 2002; Blais et al., 2004), quantum dots (Loss and DiVincenzo, 1998), and photonic systems (Aspuru-Guzik and Walther, 2012). Among these systems, superconducting qubits are one of the most promising candidates due to their relatively long coherence time (Place et al., 2021) and the facilitation of high-precision quantum operations (Ding et al., 2023). By leveraging micro-nano fabrication technology, these qubits can be integrated onto a chip at a large scale. State-of-the-art superconducting quantum processors feature more than one hundred long coherence qubits (Kim et al., 2023; Xu et al., 2023). Utilizing radio-frequency microwave technology (Krantz et al., 2019), the qubits can be prepared and measured in the $|0\rangle$ or $|1\rangle$ state with high fidelity. In recent years, the coherence time of qubits has been improved from a few microseconds to several hundred microseconds (Place et al., 2021; Wang et al., 2022), enabling us to perform thousands of effective operations (quantum gates). These achievements have driven significant advancements in the use of superconducting qubits for quantum simulations.

Simulating a quantum system generally requires explicit knowledge of the system's Hamiltonian, i.e., the energy function of the system. Similar to the early development of classical computers, problems can be addressed using either analog (Cirac and Zoller, 2012) or digital methodology (Lloyd, 1996). Analog approaches involve constructing a Hamiltonian that can be analogized to the target quantum system. The final simulation results from such an approach are highly related to the degree of correspondence between the Hamiltonians of the experimental platforms and of the target system. As a result, for specific experimental platforms, the quantum systems that can be simulated are highly selective. In contrast, a digital approach involves decomposing the target system's Hamiltonian into a sequence of unitary operations (or quantum circuits), which are further decomposed into single- or two-qubit gates. Theoretically, this decomposition method is applicable to all local systems (Lanyon et al., 2011). However, the final results rely heavily on the numbers of qubits and gates, and most importantly, the performance of the quantum gates. In the early days of the field, quantum gates had relatively low fidelities, so analog quantum simulation often yielded more accurate results. But with recent improvements in the performance of two-qubit gates (Yan et al., 2018; Foxen et al., 2020; Sung et al., 2021), the digital methodology has enabled increasingly diverse quantum simulations (Mi et al., 2022b; Zhang et al., 2022; Xu et al., 2023). Moreover, a hybrid digital-analog approach allows for more precise simulation results.

The goal of this review is to introduce near-term applications of digital quantum simulation based on superconducting qubits. The remainder of this review is organized as follows: Section 2 covers the basic principles of superconducting qubits, quantum gates, and digital quantum simulation. Section 3 presents several applications of quantum chemistry. Section 4 reviews the latest experimental research on quantum matters based on digital superconducting quantum circuits. Section 5 discusses the near-term applications of combinatorial optimization and quantum machine learning. Finally, Section 6 discusses the current challenges in digital quantum simulation and provides a future outlook.

2 Basics of a superconducting qubit

2.1 Superconducting qubit

Connecting a capacitor and an inductor in parallel can produce resonance, where the energy is mutually converted between the capacitor and the inductor, similar to the exchange of kinetic and potential energies in a mechanical spring oscillator. After quantization, such a system can be described using a harmonic oscillator. However, the system's energy levels are equally spaced, making it impossible to distinguish between the lowest two levels to form a qubit. When the inductor is replaced with a sandwich-like structure in a stack of superconductor–insulator–superconductor (known as a Josephson junction), the Josephson effect occurs. Due to the nonlinear characteristics of the Josephson junction, the energy difference between the lowest two levels differs from that of the adjacent higher levels (Clarke et al., 1988). Thus, the lowest two energy levels can be defined as the $|0\rangle$ and $|1\rangle$ states of a qubit. The effective inductance of the Josephson junction is determined by its resistance, which, along with the planar capacitor, sets the energy difference ω_{01} between $|0\rangle$ and $|1\rangle$ of the qubit, also called the resonance frequency.

When the capacitance is low, tiny electron noise can cause frequency variations that lead to decoherence. Similarly, low inductance makes the qubit more sensitive to flux noise. The ratio between these two quantities determines the qubit type. Of all types, the transmon configuration is commonly used, whose inductive energy is tens of times higher than its capacitive energy (Koch et al., 2007). To flexibly control the frequency of the qubit, practitioners generally replace the single Josephson junction with two parallel junctions, forming a superconducting quantum interference device (SQUID) used to adjust the inductance, which in turn adjusts the resonance frequency. This tunability allows convenient control of the qubits.

By connecting qubits and other components through capacitive elements, qubit control and readout can be achieved. A single-qubit state can be represented using a Bloch sphere, and thus single-qubit operations can be categorized into rotations around the *x*-, *y*-, and *z*-axes. Capacitively coupling a qubit with external microwave driving and altering the driving strength can lead to rotations around the *x*-axis, shifting the driving signal phase by 90° enables rotations around the *y*-axis, and tuning the qubit's frequency through flux lines enables rotations around the *z*-axis. Additionally, adjusting the driving phase can enable a virtual-*z* rotation. The state projection of a qubit can be measured by the capacitively connected readout resonator's frequency shift, referred to as the "dispersive shift" (Schuster et al., 2005; Krantz et al., 2019).

2.2 Quantum logic gates

Typically, the state of an arbitrary quantum system is represented by a vector. For instance, the single-qubit basic states of $|0\rangle$ and $|1\rangle$ can be represented as $[1, 0]^{\mathrm{T}}$ and $[0, 1]^{\mathrm{T}}$, respectively. The two-qubit basic states of $|00\rangle$, $|01\rangle$, $|10\rangle$, and $|11\rangle$ are represented as $[1, 0]^{\mathrm{T}}$, $[0, 1, 0, 0]^{\mathrm{T}}$, $[0, 0, 1, 0]^{\mathrm{T}}$, and $[0, 0, 0, 1]^{\mathrm{T}}$, respectively. Note that the qubit can be in a superposition state, such as $a|0\rangle+b|1\rangle$, where a and b are arbitrary complex numbers with $|a|^2+|b|^2=1$. When there are N particles, the total number of basic states will be 2^N, which is known as the exponential explosion; this computational complexity is impossible for classical computers to handle. Applying quantum gates to quantum states enables digital quantum simulation. Quantum gates are typically written in the form of a unitary matrix. For example, the quantum NOT gate can be denoted as $\boldsymbol{X}=[0, 1; 1, 0]$, which can transform $|0\rangle$ to $|1\rangle$ and vice versa. An essential single-qubit gate for swapping between basic and superposition states is the Hadamard gate $\boldsymbol{H}=\frac{1}{\sqrt{2}}[1, 1; 1, -1]$, which converts $|0\rangle$ into $|0\rangle+\mathrm{i}|1\rangle$ (i represents the imaginary unit) and vice versa.

Two-qubit gates are depicted as 4 by 4 matrices. For example, the widely used controlled-NOT (CNOT) gate (Xu K et al., 2021) is represented as:

$$\boldsymbol{U}_{\mathrm{CNOT}}=\begin{bmatrix}1 & 0 & 0 & 0\\ 0 & 1 & 0 & 0\\ 0 & 0 & 0 & 1\\ 0 & 0 & 1 & 0\end{bmatrix}, \tag{1}$$

where $|00\rangle$ and $|01\rangle$ are left unchanged, but $|10\rangle$ is switched to $|11\rangle$ and $|11\rangle$ is switched to $|10\rangle$. Any physical Hamiltonian can be implemented through universal quantum gates. However, the universal quantum gate set usually only consists of single- and two-qubit gates, with more complex quantum gates being approximated through combinations of these basic gates. One universal quantum gate set is composed of X, Y, Z, CNOT, and phase shift gates. The significance of the phase shift gates lies in the fact that other gates belong to the Clifford group, which can be effectively simulated by classical computers in polynomial time.

Capacitive coupling of superconducting qubits with externally-driven microwaves allows the execution of arbitrary single-qubit gates; this is accomplished by modulating the amplitude and phase of the microwave pulses. Two-qubit gates are realized through energy exchange by tuning the frequencies of coupled qubits until they reach resonance. The interaction between two qubits can be accomplished through capacitance, which can be replaced with tunable couplers to improve the fidelity of single- and two-qubit gates (Yan et al., 2018). Such improvement is primarily due to the suppression of coupling between neighboring qubits during single-qubit operations, as well as the reduction of leakage error by engineering of the coupler's waveform. Moreover, energy transfer between two qubits can result in two-qubit gates (Krantz et al., 2019), such as swapping $|01\rangle\leftrightarrow|10\rangle$ to execute the iSWAP gate and exchanging $|11\rangle\rightarrowtail|20\rangle\rightarrowtail|11\rangle$ to implement the CPHASE gate. Two-qubit gates can also be realized by applying microwave drives on two adjacent qubits, albeit with

extended gate times. Current quantum processors support dozens to hundreds of qubits. High-density integration of qubits, couplers, and other components employs flip-chip 3D packaging and advanced through-silicon via (TSV) technology, facilitating the future scalability of quantum processors.

2.3 Digital quantum simulation

Quantum simulation aims to map a target quantum system to a quantum simulator so that we can emulate and understand the generic quantum system in a controllable manner. Implementation of such a methodology in a programmable and digital strategy is referred to as digital quantum simulation.

To implement digital quantum simulation, we need to construct a quantum circuit consisting of three main components: initial state preparation, unitary quantum evolution, and measurement, as depicted in Fig. 1a. Take the simplest example of two spin-1/2 particles, where only XY interaction exists. The spins can be directly mapped to the states of qubits ($|\uparrow\rangle$ maps to $|0\rangle$ and $|\downarrow\rangle$ maps to $|1\rangle$). Initially, to prepare an antiferromagnetic state ($|\uparrow\downarrow\rangle$), we can apply an X gate to either of the qubits. Then, to realize XY interaction, a two-qubit iSWAP gate can be applied between them. Lastly, we can obtain the spin direction by measuring the z-axis projection of the qubits. Usually, a quantum circuit can be characterized in terms of the number of qubits, the number of quantum gates, and the depth of the quantum circuit. As depicted in Fig. 1b, some unitary operations can be decomposed into periodic circuits, such as cross-entropy benchmarking (XEB) (Arute et al., 2019) and Floquet engineering (Zhang et al., 2022). In these applications, each period is referred to as a cycle, and the total number of layers of simultaneously applied gates is referred to as the depth of the circuits. Note that in some literature, depth is also used to describe the number of layers in a unitary operator.

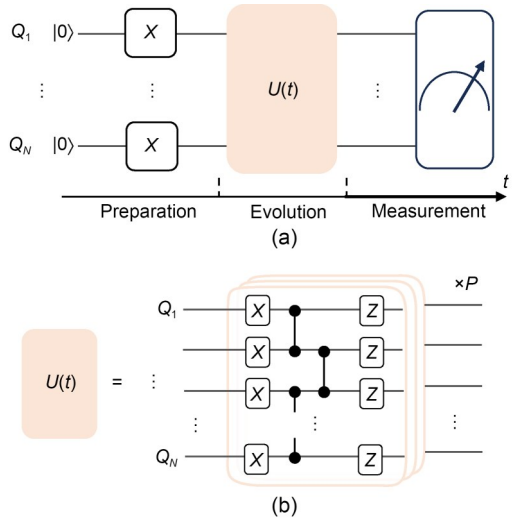

Fig. 1 Digital quantum simulation: (a) schematic of the quantum simulation, which involves three steps, i.e., preparation, evolution, and measurement (the initial state is prepared by applying the single-qubit rotation gate, such as X gate, to the corresponding qubit Q_i in the ground state $|0\rangle$; after that, the system experiences unitary evolution $U(t)$ governed by the unitary Hamiltonian; finally, as the evolution ends, the system's state should be measured, as the meter-like box indicates); (b) an example of the digital quantum circuits with P cycles of the unitary Hamiltonian $U(t)$ (each digital cycle contains two layers of single-qubit gates and two layers of two-qubit gates, serving as the local time Hamiltonian)

For more general quantum systems, the above processes are significantly more complex. Initial states in complex superpositions and entanglements are challenging to prepare, which can even nullify the advantages of quantum simulation. For more general interaction Hamiltonians, representation using quantum gates can be difficult. The Suzuki-Lie-Trotter (Trotter, 1959; Suzuki, 1976) decomposition offers an efficient means of breaking down the unitary evolution operator into a series of individual terms H_l, each capturing local interactions within a short time interval Δt. This decomposition is mathematically expressed as $U(\Delta t) = \exp\left(-\frac{\mathrm{i}}{\hbar}\sum_{l}^{L} H_l \Delta t\right)$, where L is the total number of local interactions, l is the index of local interaction, and $\hbar$ is the reduced Planck constant. As the time interval Δt approaches zero, indicating a significant increase in the number of quantum gates, the results of the decomposition gradually converge towards the actual evolution states. This approach is generally utilized to decompose the time evolution operator U into a sequence of single- and two-qubit gates, as in the example presented in Fig. 1b. However, it should be emphasized that finding an efficient decomposition in terms of universal gates is a tough task. Lastly, measuring the full information of a circuit requires the use of quantum state tomography, which is impractical for a system with more than a dozen qubits. Fortunately, there is usually no need for full information for specific problems, and local observables are often convenient and satisfactory.

Due to the fact that any unitary operation can be characterized by universal quantum gates, it is generally accepted that digital quantum simulation is universal.

In reality, only the finite-dimensional local Hamiltonian can be effectively simulated by digital quantum simulation (Georgescu et al., 2014).

3 Quantum chemistry

Chemistry simulation is commonly performed to determine the electronic structure of a molecule, which can inform ideas for new functional molecules or chemical reactions (McArdle et al., 2020). For classical computers and algorithms, it is difficult to calculate the exact properties of large molecules, and many approximations need to be adopted to simplify the evolution of the full many-body wavefunction and dynamics. Fortunately, describing the full space of the many-body wavefunction and dynamics is the merit of quantum computation and simulation. This can provide insight into quantum chemistry by simulating the ground-state energy of molecules and even the dynamics of chemical reactions. There are several algorithms for implementing quantum chemical simulation, such as the variational quantum eigensolver (VQE) (O'Malley et al., 2016; Kandala et al., 2017, 2019; Colless et al., 2018; Ganzhorn et al., 2019; Sagastizabal et al., 2019; Google AI Quantum and Collaborators et al., 2020; Heya et al., 2023; Guo SJ et al., 2024), the quantum phase estimation algorithm (QPE) (O'Malley et al., 2016; O'Brien et al., 2019), and the quantum Monte Carlo (QMC) simulation (Huggins et al., 2022), whose performances are summarized in Table 1. In the following sections, we introduce the VQE, QPE, and QMC to reveal their applications for molecular simulations.

3.1 Canonical algorithms for quantum chemistry

The VQE algorithm (McArdle et al., 2020) is built to find the ground-state energy of a given molecular Hamiltonian, H_{M}. According to the Ritz variational principle, the ground-state energy, E_0, must obey

$$E_0 \leq \frac{\langle\varphi|H_{\mathrm{M}}|\varphi\rangle}{\langle\varphi|\varphi\rangle}, \tag{2}$$

where $|\varphi\rangle$ is the trial quantum state. This indicates that VQE aims to find the minimum expectation value of H_{M} via variations of $|\varphi\rangle$. Exemplary quantum circuits of VQE can be found in Fig. 2, which consist of several steps: trial state preparation with parameterized ansatz, expectation value measurement, and parameter optimization. The hybrid quantum-classical architecture, wherein one uses a quantum processor in tandem with a classical optimizer, exploits the available quantum resources to the highest extent, while outsourcing the optimization task to a classical optimizer. Nowadays, VQE has become a popular algorithm for molecular simulations due to the parallel development of high-fidelity quantum gates.

QPE (Aspuru-Guzik et al., 2005; McArdle et al., 2020) is a traditional algorithm requiring an initial state that has a large overlap with the ground state, as well as fully coherent evolution, so that the eigenvalue of the unitary operator can act as a phase. Moreover, QPE requires deep circuits in order for the controlled evolution to approach sufficient accuracy. QPE has been utilized to simulate the energy surface of H_2 (O'Malley

Table 1 Main algorithms implemented in superconducting digital quantum simulators for quantum chemistry

Algorithm	Molecule	Maximum number of qubits	Chemistry accuracy	Reference
QPE	H_2	2	No	O'Malley et al., 2016
QMC	H_4	8	Yes	Huggins et al., 2022
QMC	N_2	12	No	Huggins et al., 2022
QMC	Diamond	16	No	Huggins et al., 2022
QMC	H_2	4	Yes	Kandala et al., 2017; Guo SJ et al., 2024
VQE	LiH	6	Yes	Kandala et al., 2017; Guo SJ et al., 2024
VQE	BeH	6	Yes	Kandala et al., 2017
VQE	H_6, H_8	6, 8	Yes	Google AI Quantum and Collaborators et al., 2020
VQE	F_2	12	No	Guo SJ et al., 2024
VQE	H_{10}, H_{12}	10, 12	No	Google AI Quantum and Collaborators et al., 2020

Chemistry accuracy benchmarks the experimentally simulated accuracy of the ground-state energy achieving the level of chemistry accuracy (Yes) or not (No), where chemistry accuracy is approximated 1.6×10^{-3} Hartree or 1 kcol/mol or 0.043 eV

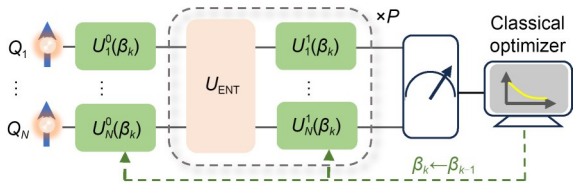

Fig. 2 Quantum circuits of VQE. There are three steps for performing the quantum-classical hybrid QVE: trial state preparation with variational ansatz, expectation value measurement, and parameter optimization and feedback. The first step is accomplished by the parameterized ansatz, which is composed of local single-qubit rotation operators ($U_i^0(\beta_k)$, $U_i^1(\beta_k)$), parameterized by phase β and the two-qubit gates associated with the entanglement operator U_{ENT}. The subsequent measurement obtains the expectation value of H, which is transferred to the classical optimizer to yield the optimized parameters β for the next iteration, according to descent optimization algorithms. P is the number of cycles of the parameterized circuits within the dashed box

et al., 2016). However, the estimated accuracy of the ground-state energy is still far from the desired accuracy for chemistry applications (about 1.6×10^{-3} Hartree).

QMC (Foulkes et al., 2001) aims to approach the exact ground state under quantum imaginary-time evolution (QITE) (Motta et al., 2020) of an initial state, with nonzero overlap with the ground state. Classical Monte Carlo simulation is bounded due to the sign problem, leading to divergence when simulating fermions. However, the version of QMC with unbiasing fermions associated with QITE showcased promising results in simulating N_2 molecules in 12-qubit and diamond in 16-qubit superconducting chains (Huggins et al., 2022).

3.2 Experimental progress

O'Malley et al. (2016) first implemented the VQE algorithm in a 2-qubit superconducting system to simulate the surface energy of H_2 with robustness to certain errors. The accuracy of simulating the ground-state energy of H_2 employing VQE reaches the so-called chemical accuracy, which is the level required to make realistic predictions. Later, Kandala et al. (2017) from IBM implemented a hardware-efficient ansatz preparation for VQE in a 6-qubit superconducting chain to simulate the ground-state energies of H_2, LiH, BeH_2, and quantum magnets with a shallow quantum circuit. Additionally, Colless et al. (2018) experimentally demonstrated an augmented VQE that uses a polynomial number of additional tomographic measurements to extract molecular excited-state energies of H_2 based on the quantum subspace expansion. This showed that the effects of incoherent errors could be mitigated by their extended protocol. Kandala et al. (2019) also showcased a mitigation protocol for incoherent errors in a 4-qubit system via perfect energy simulation of H_2 and LiH, which enhanced the computational capability of superconducting qubits without requiring more sophisticated hardware.

The emergence of Sycamore in 2019 has led to significant progress. Google AI Quantum and Collaborators et al. (2020) reported two applications of quantum chemistry using up to 12 qubits in Sycamore via VQE with Hartree-Fock ansatz, as shown in Fig. 3a. This includes simulating the binding energy of hydrogen chains with qubit numbers from 6 to 12 (Fig. 3b), as well as modeling the isomerization mechanism of diazene (Fig. 3c). In terms of more complex molecules investigated in the Sycamore processor, Tazhigulov et al. (2022) studied the simulation of the finite-temperature dynamic correlation function of Fe-S clusters in 4-qubit and 8-qubit systems, as well as α-$RuCl_3$ in 6-qubit and 10-qubit systems, associated with ancilla qubit and QITE. Another ansatz called the unitary-coupled cluster (UCC) (Bartlett et al., 1989; Romero et al., 2019; Anand et al., 2022; O'Brien et al., 2023) also improved the chemistry accuracy with a deep quantum circuit. Guo SJ et al. (2024) demonstrated the implementation of VQE with UCC for H_2, LiH, and F_2 from 4 to 12 qubits on the superconducting quantum processor Zuchongzhi 2.0; chemical accuracies for H_2 (at all bond distances) and LiH (at small bond distances) were obtained, but not for the large molecule of F_2. In the experiments, to both reduce the complexity of UCC and guarantee accuracy, an effective symmetry verification of the particle number parity was employed. The ansatz of unitary pair-coupled-cluster doubles (O'Brien et al., 2023) was also effectuated for simulating the Richardson-Gaudin model and a cyclobutene open ring.

In short, with the aid of high-precision manipulation of superconducting quantum circuits and generalized optimization algorithms, the chemistry accuracy of the ground state of small molecules can be obtained, as shown in Table 1. For more complex molecules and structures, more efficient algorithms involving a greater number of qubits and deeper logical gates are required. In addition to the ground state, for chemical dynamics properties, Huang et al. (2022) implemented the first simulation of the linear response properties of molecules, such as H_2 and carbon monoxide, using the variational quantum response algorithm with shallow superconducting circuits. Their results revealed the ability

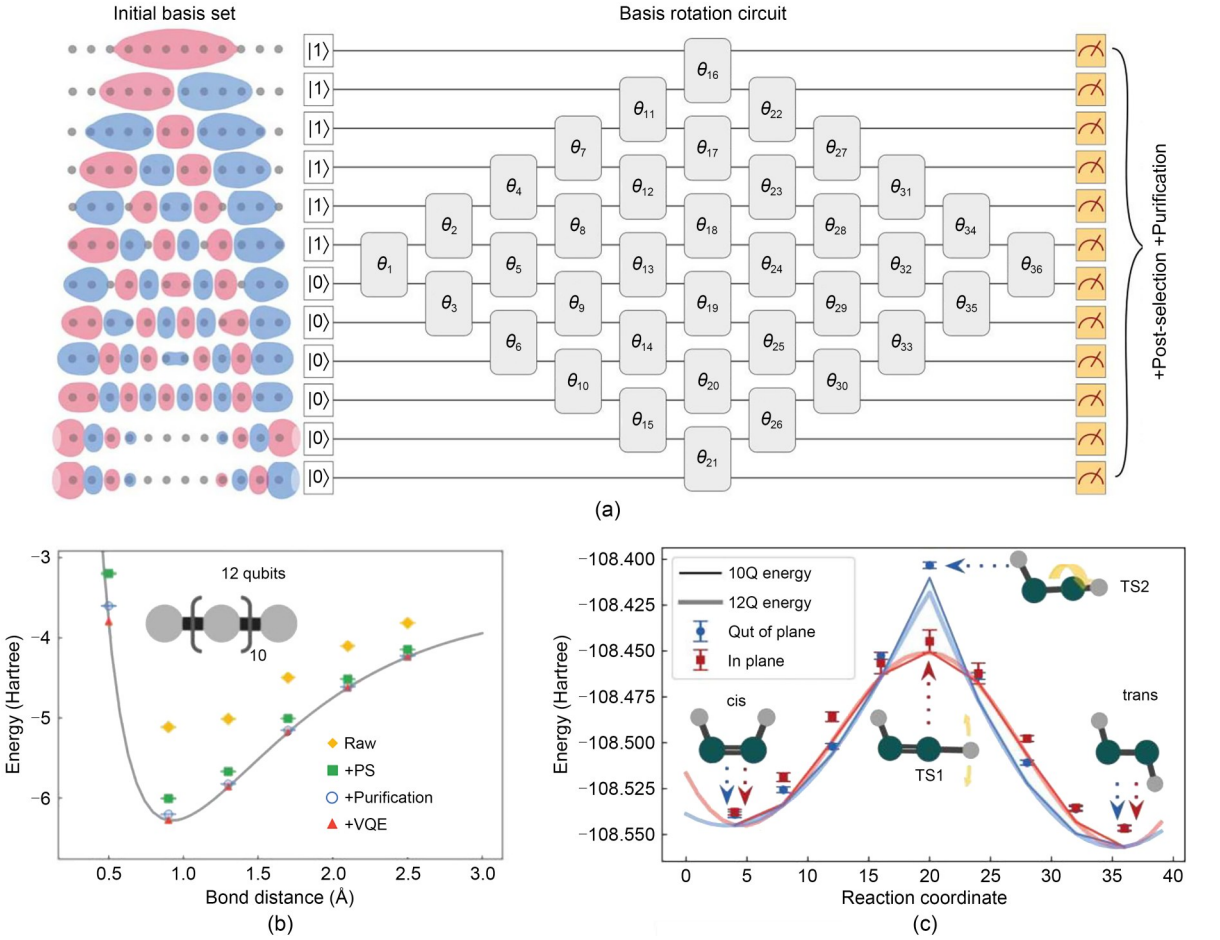

Fig. 3 Performance of VQE with Hartree-Fock ansatz for quantum chemistry: (a) application of quantum chemistry using 12 qubits (the left panel is the initial basis set describing the initial orbitals for the H_{12} chain with electron-electron interactions; the right panel of the circuit diagram captures the basis rotation ansatz for a chain of 12 hydrogen atoms, where the gray box labeled as rotation angle θ_i is the set of two-qubit gates and single-qubit rotation gates with the angle of $-\theta$ and $\theta+\pi$); (b) binding curve simulation results for H_{12} with various types of error mitigation (the raw data (yellow diamonds), applying postselection (+PS, green squares), and applying PS and purification (+Purification, blue circles) are computed from a classical simulation with optimal θ_i; +VQE (red triangles) means applying PS, purification, and variational relaxation); (c) Hartree-Fock curves for diazene isomerization between 'cis' and 'trans' configurations with different reaction coordinates (TS1 (with red curves and points) and TS2 (with blue curves and points) correspond to the in-plane and out-of-plane rotated transition states, respectively; the nine points along the reaction paths are obtained from Sycamore with VQE; the solid line and corresponding transparent line stand for the simulated energy of the 10-qubit (10Q) and 12-qubit (12Q) systems, respectively). Reprinted from (Google AI Quantum and Collaborators et al., 2020), Copyright 2020, with permission from the American Association for the Advancement of Science. References to color refer to the online version of this figure

of superconducting quantum techniques to simulate dynamic properties.

4 Quantum matters

Various physics models have been developed to study quantum matters, such as the Hubbard model, the Ising model, the Heisenberg model, and the Kitaev model, which are all accessible for digital quantum simulation. Here, we introduce several canonical models and explore practical implementations of nonequilibrium many-body physics and the topological phase of matter with digital quantum simulation. In Table 2, we list some implementations of quantum matters associated with superconducting digital quantum simulation.

4.1 Typical models

The Hubbard model (Arovas et al., 2022; Qin et al., 2022) is a pivotal framework for elucidating the

Table 2 Main condensed matters implemented by the digital superconducting quantum circuits

Model	Phase of matter	Maximum number of qubits	$\mathcal{F}_{1Q}$, $\mathcal{F}_{2Q}$	Total duration (μs)	Reference
Hubbard	TPs	16	0.999, 0.990	About 6	Koh et al., 2022a
Ising	QMBS	19	0.999, 0.984	About 32	Chen et al., 2022
Ising	SPT	47	0.999, 0.994	About 28	Mi et al., 2022a
Heisenberg	Magnets dynamics	46	0.999, 0.994	About 3	Rosenberg et al., 2024
Floquet	MBL-DTC	20	0.9992, 0.9890	About 6	Mi et al., 2022b
Floquet	Scar DTC	60	0.999, 0.995	About 15	Bao et al., 2024
Toric-code	Anyons	68	0.9991, 0.9940	About 1	Xu et al., 2023

TPs: topologically ordered phases of matter without symmetry protection; QMBS: quantum many-body scars; SPT: symmetry-protected topological states; MBL-DTC: many-body localized discrete time crystal; Scar DTC: Scar discrete time crystal. $\mathcal{F}_{1Q}$ and $\mathcal{F}_{2Q}$ denote the average fidelities of single- and two-qubit gates, respectively, adopted from the works with the maximum number of qubits. Total duration refers to the longest time of the digital circuit sequences

conducting properties of solid-state matters with strong correlations. At low temperatures, electron wave functions in tight-binding states predominantly localize around atomic nuclei, but have the potential to hop to adjacent nuclei. The system's Hamiltonian can be written as:

$$H_{\text{Hubbard}}=-V\sum_{\langle i,j,\sigma\rangle}\left(b_{i\sigma}^{\dagger}b_{j\sigma}+b_{j\sigma}^{\dagger}b_{i\sigma}\right)+U\sum_{i}n_{i\uparrow}n_{i\downarrow}, \quad (3)$$

with the hopping strength V, the repulsion strength U, the fermionic annihilation (creation) operator b ($b^{\dagger}$), the number operator $n=b^{\dagger}b$, and i and j covering all adjacent sites, as well as $\sigma\in\{\uparrow,\downarrow\}$. Barends et al. (2015) implemented the fermionic Hubbard model with up to four fermionic modes with superconducting quantum circuits. In excess of 300 single-qubit and two-qubit CZ gates were employed to implement the required separately tunable XX, YY, and ZZ couplings. Practically, U is considered by the anharmonicity of the qubit, to wit, $U\propto\omega_{21}-\omega_{10}$. For a transmon qubit, $U\sim-200\times2\pi$ MHz.

The Heisenberg model captures the behavior of a variety of quantum materials, including magnetic crystals, low-dimensional magnets, and 2D layered materials. The 1D Heisenberg model is given as:

$$H_{\text{Heisenberg}}=-\sum_{i}\left(J_x\sigma_i^x\sigma_{i+1}^x+J_y\sigma_i^y\sigma_{i+1}^y+J_z\sigma_i^z\sigma_{i+1}^z+h_z\sigma_i^z\right), \quad (4)$$

where J_δ ($\delta\in\{x, y, z\}$) is the strength of the corresponding exchange couplings, h_z refers to the strength of an external magnetic field, and σ_i is the element with local index i of the Pauli matrix. This model describes nearest neighbor exchange interactions between spin-1/2 particles. As $J_x=J_y=J_z$, the Heisenberg model describes quantum magnetism with a global SU(2) symmetry. Otherwise, it can be derived to the transverse Ising model with $J_y=J_z=0$, the XY model with $J_z=0$, and the XXZ model with $J_x=J_y\neq J_z$. Salathé et al. (2015) simulated the spin dynamics of the Heisenberg and Ising spin models in two transmon-qubit systems with two-qubit SWAP gates for XY interactions. The intricate spin dynamics of a larger 1D system for the XXZ model had been emulated in a superconducting chain with 46 qubits (Rosenberg et al., 2024), where the spin model was implemented by periodic application of two-qubit unitary fSim gates with low error rates (Foxen et al., 2020).

The Kitaev model (Kitaev, 1997) was initially proposed to describe a spin liquid state in frustrated magnetic systems. However, it has also been adapted to describe unconventional superconductivity and topological phases of matter with long-range entanglement (Kitaev and Preskill, 2006; Wen, 2017). The Hamiltonian of the 1D Kitaev chain can be written as:

$$\begin{aligned}H_{\text{Kitaev}}=&-\mu\sum_{i}c_i^{\dagger}c_i-V_{\text{t}}\sum_{\langle i,j\rangle}\left(c_i^{\dagger}c_j+c_j^{\dagger}c_i\right)-\\&\Delta e^{i\phi}\sum_{\langle i,j\rangle}\left(c_ic_j+c_i^{\dagger}c_j^{\dagger}\right),\end{aligned} \quad (5)$$

where fermionic operators c_i and $c_i^{\dagger}$ represent the creation and annihilation of electrons at site i, μ is the chemical potential, V_{t} is the tunneling strength between nearest neighbor sites, and Δ and ϕ denote the superconducting pairing strength and phase, respectively. As $\Delta=V_{\text{t}}\neq0$ and $\mu=0$, by introducing two Majorana operators ($\gamma_{A,i}$ and $\gamma_{B,i}$) for a fermion operator $c_i=e^{-i\phi}(\gamma_{B,i}+i\gamma_{A,i})/2$,

the model reduces to a topological phase characterized by the presence of Majorana edge modes (MEMs) (Kitaev, 2001; Sarma et al., 2015), which are localized at the boundaries of the systems with zero energy. MEMs hold unique properties, such as robustness to certain perturbations, making them promising candidates for topological quantum computing (Stern and Lindner, 2013; Sarma et al., 2015; Lian et al., 2018).

4.2 Experimental progress

Analog quantum simulation has played a critical role in exploring nonequilibrium many-body physics (Yao and Xiang, 2024) and topological phases of matters (Roushan et al., 2014; Schroer et al., 2014; Tan et al., 2017, 2018, 2019), for the tunable and strong coupling between superconducting qubits. However, for more complex and high-precision controlling, such as Floquet systems, digital quantum circuits can provide more compelling results. Here, we highlight several promising experiments implemented by superconducting digital quantum circuits, including discrete time crystals (DTCs) and topological orders.

4.2.1 Nonequilibrium many-body physics

Emerging DTC (Else et al., 2020, 2016) is an out-of-equilibrium phase of matter with broken discrete time-translation symmetry by Floquet driving, which holds π-periodic eigenenergies. The hallmark of DTC is the oscillation of local observables in a period twice that of the Floquet drive (U_F), irrespective of the initial state, which is predicted to survive in the ergodicity-breaking system (Else et al., 2016; Yarloo et al., 2020; Bluvstein et al., 2021; Maskara et al., 2021) or prethermalization system (Else et al., 2017; Machado et al., 2020; Kyprianidis et al., 2021). Here, we focus on the ergodicity-breaking protected DTC, because of their extensive progress in superconducting digital quantum simulation applications. The Hamiltonian of the many-body localization-protected DTC with Floquet driving is given as (Else et al., 2016):

$$H_F=\begin{cases} H_{MBL}=\sum_i (J_i\sigma_i^z\sigma_{i+1}^z+h_i\sigma_i^z), & 0<t<t_0, \\ H_{Flip}=g\sum_i \sigma_i^x, & t_0<t<t_0+t_1, \end{cases} \tag{6}$$

where H_{MBL} ensures the eigenstates of individual σ_i^z avoiding thermalization, H_{Flip} rotates spins with an angle of gt_1, and g is the rotation rate. The period of such Floquet driving is $T=t_0+t_1$. Specifically, in H_F, parameters J and h are drawn from certain random distributions. As $t_0=t_1=\pi/(2g)$, H_{Flip} effectively functions as a π pulse, resulting in a doubled periodicity of local observables. This scenario makes the disordered Floquet system remarkably resilient to minor perturbations, maintaining a robust subharmonic response even with minor variations in initial states and Hamiltonian perturbations.

Many-body localized discrete time crystal (MBL-DTC) has been implemented by various quantum simulators (Zhang et al., 2017; Xu HK et al., 2021; Frey and Rachel, 2022; Mi et al., 2022b). Ippoliti et al. (2021) pointed out that the genuine MBL-DTC can be implemented in superconducting quantum simulators with digital circuits due to its controllable short-range interactions, Ising-even disorder, and various initial states. Recently, the Google AI team (Mi et al., 2022b) implemented MBL-DTC with a 20-qubit chain isolated from the Sycamore processor with deep digital quantum circuits. The Floquet drive consisted of longitudinal fields, Ising couplings, and imperfect global spin flips. The first and last terms are implemented by simultaneous Z gate and X gate, respectively, as shown in Fig. 4a. The strong and disordered Ising-even couplings are controlled by the two-qubit controlled-phase gates. The subharmonic oscillation of the autocorrelator persists for up to 100 cycles of the Floquet drive (Fig. 4b). Moreover, by tuning the parameter g of H_{Flip} in Eq. (6), a phase transition from DTC to thermalization was observed. On the other hand, Xu HK et al. (2021) and Frey and Rachel (2022) realized the DTC through an analogous strategy in superconducting qubit chains, where the long-time stroboscopic dynamics and signatures of crossover between the DTC and thermal phase were revealed.

Meanwhile, Zhang et al. (2022) successfully implemented 1D Floquet symmetry-protected topological phases (FSPT), also known as topological DTCs, on a 26-qubit superconducting chain, as depicted in Figs. 4c and 4d. In particular, the Floquet Hamiltonian consists of two parts: $H_1=\sum_k(\pi/2-\xi)\sigma_k^z$ and $H_2=\sum_k(J_k\sigma_{k-1}^z\sigma_k^x\sigma_{k+1}^z+V_k\sigma_k^x\sigma_{k+1}^x+h_k\sigma_k^x)$, where k is the qubit index, J_k is the three-body interaction strength, and ξ, V_k, and h_k refer to the various perturbations. Such Hamiltonian features with $\mathbb{Z}_2\times\mathbb{Z}_2$ symmetry and the discrete time-translational symmetry in this phase are preserved

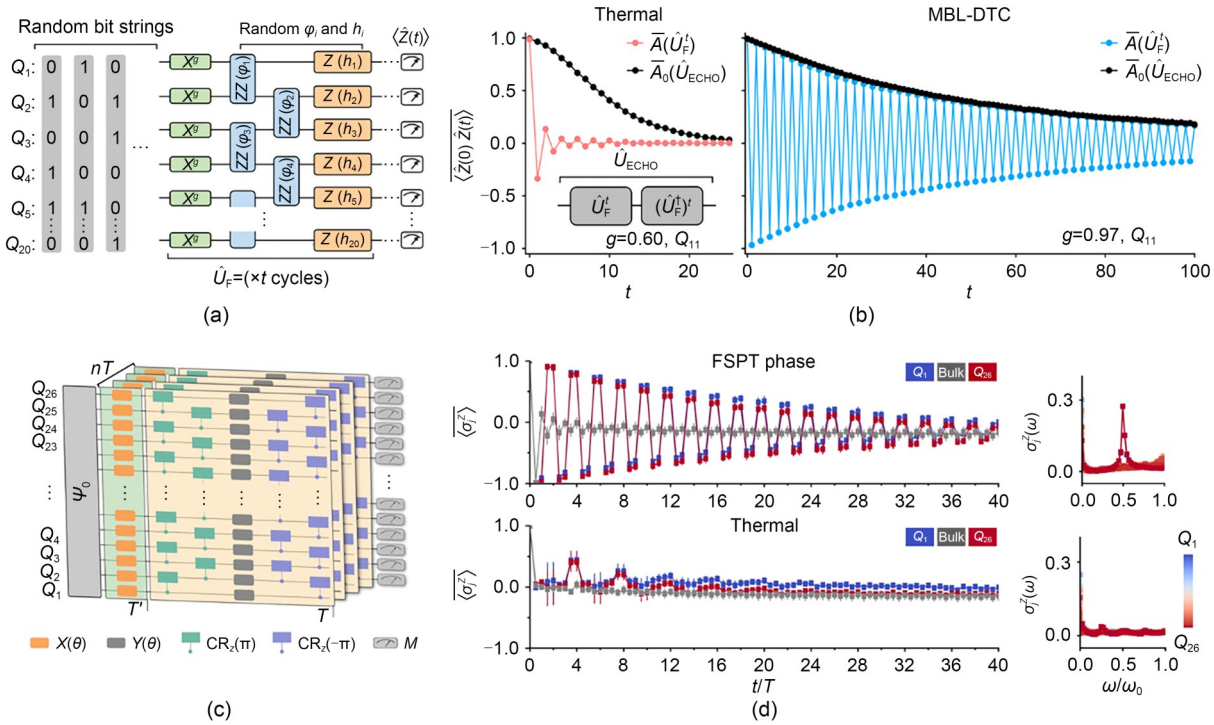

Fig. 4 Digital quantum simulation of the DTC: (a) digital quantum circuits for implementing the MBL-DTC, where random bit strings stand for the initial state for various realizations and the Floquet unitary U_F involves disordered single-qubit gates and controlled-phase gates; (b) experimental results of the averaged autocorrelators $\bar{A}=\overline{\langle Z(0)Z(t)\rangle}$ at qubit Q_{11} provided for the thermal phase (g=0.6, left panel) and the MBL-DTC phase (g=0.97, right panel) (each phase has been explored in the Floquet circuits ($\bar{A}(U_F^t)$) and the echo circuits ($\bar{A}_0(U_{ECHO}^t)$), and the echo circuit $U_{ECHO}=(U_F^\dagger)^t U_F^t$ reverses the evolution of Floquet after t cycles, which can help quantify the impact of decoherence); (c) schematic illustration of the experimental circuits to achieve the Hamiltonian of the Floquet symmetry-protected topological phases with an evolution time of nT (Ψ_0 is the initial state of system, $X(\theta)$ refers to the X gate, and M represents the measurement); (d) experimental results of dynamics and the Fourier transform of disorder-averaged local magnetization $\langle\sigma_j^z\rangle$ in the FSPT phase (top panel) and thermal (bottom panel). Figs. 4a and 4b are reprinted from (Mi et al., 2022b), Copyright 2022, with permission from Springer Nature; Figs. 4c and 4d are reprinted from (Zhang et al., 2022), Copyright 2022, with permission from Springer Nature. References to color refer to the online version of this figure

in the bulk, with disruptions occurring at the boundaries. Experimentally, the three-body interactions were implemented by structuring sandwich-like circuits $CR_z(\pm\pi)$–$Y(\theta)$–$CR_z(\pm\pi)$, where $CR_z(\pm\pi)$ is the combination of a two-qubit CZ gate and a virtual Z gate, and $Y(\theta)$ is the single-qubit Y gate with phase θ. Moreover, the robustness of the FSPT phase to the symmetry-preserving noise was demonstrated. Fundamentally, the FSPT phase is safeguarded by the engineered many-body localization, ensuring its robustness regardless of boundary or bulk effects. Additionally, Ying et al. (2022) investigated the Floquet prethermalization protected by approximate U(1) symmetry with digital-analog quantum simulations, where the averaged magnetization oscillates subharmonically with a prolonged lifetime as the Ising interactions turn on. However, it is hard to consider this as a pure prethermal DTC, due to the obstacle of technical control of long-range interactions, which is critical to the realization of prethermal DTC (Else et al., 2020; Machado et al., 2020).

Beyond the strong ergodicity-breaking like MBL, the weak ergodicity-breaking, such as quantum many-body scar (QMBS) (Turner et al., 2018; Serbyn et al., 2021), sheds light on safeguarding DTC (Bluvstein et al., 2021). QMBS is achieved with the decoupled subregion of eigenstates, which circumvents the eigenstate thermalization hypothesis (ETH). QMBS is expected to exhibit resilience against perturbations and abundant entanglement architectures, which also has been implemented by digital circuits (Chen et al., 2022). These attributes render QMBS a promising candidate for deployment in quantum information processing

tasks, offering potential advantages in terms of stability and the capacity to accurately manipulate quantum states. Practically, quantum many-body scarred DTC (Yarloo et al., 2020; Haldar et al., 2021; Maskara et al., 2021) has been proposed to prepare the Floquet system within the subregions of QMBS. The hopping among QMBSs can lead to the long-lived stroboscopic dynamics of DTC. Compared to MBL-DTC, quantum many-body scarred DTC exhibits the phenomena of quantum chaos, and does not encounter the dilemmas that MBL does.

Cat scar DTC (Huang, 2023), a special kind of quantum many-body scarred DTC (Mizuta et al., 2020; Mukherjee et al., 2020; Haldar et al., 2021; Maskara et al., 2021), is proposed through the engineering of multiple pairs of cat eigenstates featuring robust Ising interactions. This system exhibits remarkable resilience against various perturbations and displays oscillatory dynamics that persist for an exponentially increasing duration. Recently, Bao et al. (2024) implemented the cat scar-enforced DTC in a 2D grid superconducting simulator with qubit numbers up to 60. The implementation involved a Floquet drive unitary, characterized by two-qubit CZ gates serving as Ising couplings, complemented by random single-qubit gates. Practically, the cat scar DTC was leveraged to prolong the lifetime of a generic Greenberger-Horne-Zeilinger (GHZ) state. This application not only underscores the potential of DTCs for quantum information processing, but also opens novel avenues for the preparation of large-scale GHZ states.

4.2.2 Topological phase of quantum matters

MEMs (Kitaev, 2001) emerge in the boundaries of 1D topological phase systems, which can be well described by the Kitaev model. Due to the degeneracy of MEMs, they are thought to be immune to local parity-preserving noise. Mi et al. (2022a) simulated MEMs with a 47-superconducting-qubit chain under a drive composed of quantum circuits for a kicked Ising model. Meanwhile, the Kitaev model was mapped to a transverse Ising spin model with $\mathbb{Z}_2$ parity symmetry via a Jordan-Wigner transformation. Each MEM also was represented by a sum of local Majorana operators. Remarkably, it was found that the symmetry protection of MEMs against noise, such as local potential perturbations, is still sensitive to the decoherence decay of transmon qubits.

Topological insulators exhibit a unique type of time-reversal symmetry, protecting topological quantum matter that behaves as an insulator in its interior, but supporting conducting states on its surface or edges. These conducting states are protected by symmetry and are immune to backscattering caused by impurities or defects, making them robust to disorders. The discovery of topological insulators has significantly expanded our understanding of electronic states in condensed matter physics and has opened up new avenues for applications in electronics and quantum computing. Experimentally, a topological insulator at finite temperature was tested by the topological Uhlmann phase simulated by a 3-qubit entangled system in the IBM quantum experience platform (Viyuela et al., 2018). The Uhlmann phase is an extension of the Berry phase of pure-state density matrices to mixed-state density matrices. By simulating the simplified two-band model of topological insulators with a qubit, and encoding the temperature of the system in the entanglement with ancilla qubits by applying CNOT gates, the topological Uhlmann phases were successfully probed. However, more deterministic and detailed simulations of topological insulators at a large scale are lacking.

Specifically, the topological order can be realized by anyonic exchange statistics of quasiparticles and long-range entanglement (Wen, 2017). To characterize the long-range quantum entanglement of a quantum system, such as the toric code (Kitaev, 2003), topological entanglement entropy (Kitaev and Preskill, 2006; Levin and Wen, 2006) is introduced as $S_{\text{topo}}=-\ln \mathcal{D}=-\ln \sqrt{\sum_q d_q^2}$, where d_q is the quantum dimension of an excitation with charge q. $\mathcal{D}$ is called total quantum dimension. Generally, S_{topo} is a topological invariant, which is merely dependent on the topology of the joined regions rather than the geometry. On the other hand, $S_{\text{topo}}<0$ is universal for topologically-ordered states. For instance, $S_{\text{topo}}=-\ln 2$ for the Abelian anyons in toric code architecture with four sectors (Kitaev and Preskill, 2006), due to d_q being 1 for any Abelian anyon. However, for non-Abelian anyons, the quantum dimension d_q is greater than 1. The main challenge for the implementation of a topological order state is the generation of long-range entanglement. The topological entanglement entropy was probed by Satzinger et al. (2021) on a 2D 31-qubit lattice for testing the topological nature of the toric code eigenstates. Later,

non-Abelian braiding of anyons was investigated in larger-scale lattices with surface code (Google Quantum AI and Collaborators, 2023), a toric code model (Xu et al., 2023), and a Fibonacci string-net model (Xu SB et al., 2024).

Furthermore, thanks to the accessibility of noisy quantum simulators from IBM, many explorations of novel quantum matters have been carried out with digital quantum circuits, such as Chern topological states (Koh et al., 2022a), fractional quantum Hall states (Rahmani et al., 2020; Kirmani et al., 2022), and other emerging symmetry-protected topological states (Choo et al., 2018; Azses et al., 2020; Koh et al., 2022b; Smith et al., 2022). Furthermore, we note that there exist other cloud platforms based on superconducting qubits (Jin et al., 2024; Xu HZ et al., 2024). These platforms have contributed to simulating the topological phase (Xiang et al., 2023) and to machine learning applications (Wang et al., 2024).

5 Other applications

5.1 Combinatorial optimization

Combinatorial optimization (CO) has significant applications in many real-world scenarios, including the optimization of logistics and supply chains. In practice, the global solution of a CO problem is usually difficult to obtain directly due to disturbances from the massive local solutions during optimization. To overcome such obstacles associated with quantum circuits, the quantum approximation optimization algorithm (QAOA) (Farhi et al., 2014) has emerged.

QAOA can be viewed as the trotterized version of quantum annealing (Streif and Leib, 2019) with the aid of a classical quantum hybrid architecture. Generally, a QAOA contains three portions (Zhou et al., 2020): initialization, functional evolution, and classical optimization. The initial state is a symmetric superposition state. The functional evolution is the ability of the parameterized circuits to realize two-body interactions and local rotations, which contributes to the exception value of the problem-specific operator serving as the cost function. Such an estimated cost function is dissected by the classical optimizer, which then suggests new parameters according to the typical parameter optimization algorithms for reaching a minimum of the cost function. In other words, QAOA seeks the ground state of the cost function with variational waveform ansatz.

In terms of experimental implementation of QAOA in superconducting digital circuits, Otterbach et al. (2017) demonstrated the hybrid QAOA for the weighted MaxCut problem with P=1 in the Rigetti 19-qubit superconducting quantum processor. This harnesses the Bayesian optimization of variational parameters with up to 55 steps to obtain the optimal parameters. Later, Bengtsson et al. (2020) attained the QAOA with two superconducting qubits, where small instances of the NP-complete exact-cover problem were solved with a success of 0.966 with P=2 circuits. Karamlou et al. (2021) investigated the performance of variational quantum factoring (VQF) in several qubits associated with QAOA ansatz, where integer 1099551473989 is factored via 3-qubit quantum circuits with a success rate of around 0.8. Harrigan et al. (2021) executed the QAOA for three canonical problems in the Sycamore processor. The performance of such implementations decreases as the problem size increases for the Sherrington-Kirkpatrick (SK) model (Sherrington and Kirkpatrick, 1975) and the MaxCut problem (Zhou et al., 2020). Even though the performance of QAOA in the native graph of hardware grid problems with shallow depth could follow the noiseless simulation, there remains a challenge for scaling non-native graph problems.

Overall, there is still no quantum optimization algorithm implemented in superconducting quantum circuits that can significantly outperform the classical heuristic optimization. Many protocols have been proposed to reduce the depth of quantum circuits (Abrams et al., 2020; Zhou et al., 2020; Chai et al., 2022; Yu et al., 2022, 2023; Zhu LH et al., 2022) to achieve more effective applications.

5.2 Quantum machine learning

As an important branch of artificial intelligence (AI), machine learning (ML) has become a powerful tool to elucidate general patterns from limited data (Dunjko and Briegel, 2018), providing predictions for unknown data according to the learned patterns. Following the rapid progress of quantum technologies (Schuld et al., 2015; Preskill, 2018), implementing ML in the quantum domain has attracted widespread attention, and is often referred to as quantum machine learning (QML). As opposed to classical ML, QML owns more

powerful expression and stronger computing capability thanks to quantum state superposition, which has many important near-term applications in quantum devices (Biamonte et al., 2017; Ristè et al., 2017; Dunjko and Briegel, 2018). In terms of the near-term implementation of QML in superconducting circuits (Bharti et al., 2022), we mainly discuss the applications of the quantum neural network (QNN) and quantum kernel estimation (QKE) for supervised learning, as well as quantum generative adversarial network (QGAN) for unsupervised learning. The realization of reinforcement learning in superconducting circuits (Reuer et al., 2022) still needs further exploration.

5.2.1 QNN

A classical neural network (NN) is an architecture mimicking the biological neural system in terms of structure, mechanics, and functions. In practice, an NN is established by interlacing layers of linear and nonlinear functions, where the linear function can be interpreted as a full-connected layer (FC-layer) to capture the connection between the input neurons and output neurons. Learning is accomplished by training parameters in the NN. The perceptron is the earliest NN with the ability of machine learning, and has been implemented on a 2-qubit superconducting system with controlled gates by Pechal et al. (2022). Gong et al. (2023) implemented a QNN with the digital-analog quantum framework on Zuchongzhi 1.0, where the MBL states were distinguished with a success rate of ~95% when just measuring one qubit.

During training an NN based on the backpropagation and gradient methods, the loss function gradients tend to become exponentially more absent with problem size, which is known as a barren plateau (McClean et al., 2018; Wang et al., 2021). To mitigate this issue, a convolutional neural network (CNN) was introduced (Lecun et al., 1998) by selecting rectified neuron activation functions or multilayer training. Importantly, a CNN replaces the FC-layer in an NN with a convolutional layer (C-layer) to extract feature maps through a moving convolutional kernel. As a prototypical deep NN, a CNN provides a worthy architecture for image processing (Lecun et al., 1998; Krizhevsky et al., 2017) and visual recognition (LeCun et al., 2015) tasks.

Inspired by the CNN, the quantum convolutional neural network (QCNN) was proposed (Cong et al., 2019; Henderson et al., 2020; Kerenidis et al., 2020; Wei et al., 2022) for quantum phase recognition and optimizing quantum error correction (QEC). In this method, data is encoded in multiqubits as an initial quantum state, followed by quantum circuits with multilayer logical gates, and finally measurement. In 2022, the capability of the QCNN for quantum phase recognition was demonstrated by Herrmann et al. (2022) on a 7-qubit superconducting system. Specifically, the C-layer is implemented as CZ gates and the nonlinear mapping function is composed of a series of Boolean logic circuits in terms of AND and XOR gates. Finally, the enhanced performance of the QCNN was demonstrated with measured expectation values approaching 0.7 in the symmetry-protected phase, and near zero for the trial phase. This work paved the way for exploring a trainable parameterized QCNN and more complex applications for QCNNs. Moreover, the hybrid quantum-classical convolutional neural network (QCCNN) (Henderson et al., 2020; Liu et al., 2021) was proposed to reduce the size of qubits required by replacing the convolutional layer with non-parametric random quantum circuits (Henderson et al., 2020) or parameterized quantum circuits (Liu et al., 2021). Nevertheless, the application of QCCNNs in near-term quantum devices is still scarce.

5.2.2 QKE

As for binary classification problems, the perceptron (Pechal et al., 2022), support vector mechanics (SVM) (Rebentrost et al., 2014; Li et al., 2015), and the kernel method have been developed (Schuld and Killoran, 2019; Schuld, 2021). A perceptron is the simplest model for linear binary classification. SVM is a typical binary classifier, which finds a robust hyperplane for linear classification that has the maximum margin (Schuld et al., 2015). For nonlinear classification tasks, where the data shows an interlacing distribution in feature space, it can be quite challenging for SVMs. By introducing the kernel method, the datasets in feature space ($\mathcal{F}_0$) can be mapped into a higher dimensional space ($\mathcal{F}_1$) through the implicit feature mapping function of Θ, where the mapped datasets can then be linearly classified by a hypersurface. The key point is that the inner product in $\mathcal{F}_1$ between $\Theta(x_i)$ and $\Theta(x)$ can be estimated by the symmetric positive definite kernel method, which is called kernel estimation (KE) (Jerbi et al., 2023). In a quantum setting, the results of QKE could be simulated by measuring

the overlap between the pair of quantum states $|\Theta(x)\rangle$ and $|\Theta(x_i)\rangle$, which are encoded from data x and x_i, respectively.

Havlíček et al. (2019) experimentally materialized the QKE and a variational quantum classifier with two superconducting qubits, for a feature map that is hard to estimate classically. This realization enables noisy intermediate-scale quantum (NISQ) devices to fulfill and extend the application beyond binary classification for QKE. Peters et al. (2021) pushed the scalability of QKE up to 17 qubits on the Sycamore. However, it is claimed there is still an absence of quantum advantage for QKE.

5.2.3 QGAN

Generative adversarial networks (GANs) (Goodfellow et al., 2014) are a two-player minimax game obeying Nash-equilibrium conditions. It aims to generate new samples obeying the distributions of real samples via the implicit model of adversarial learning. GANs have applications in many fields, such as image generation (Salimans et al., 2016), video generation (Mathieu et al., 2016), image super-resolution (Ledig et al., 2017), and synthetic data generation (Killoran et al., 2017). In such GANs, there are parameterized discriminator networks and generator networks. QGAN is the GAN commonly considered in the quantum setting (Dallaire-Demers and Killoran, 2018; Lloyd and Weedbrook, 2018), where the data input and output are quantum state encodings in qubits, and both the generator and discriminator are implemented as quantum circuits (Dallaire-Demers and Killoran, 2018).

The first proof-of-concept experimental demonstration of QGAN in superconducting circuits was achieved by Hu et al. (2019) with a 1-qubit system. Later, Huang KX et al. (2021) materialized a QGAN in a 5-qubit superconducting system, where the generator and the discriminator were parameterized via layers of single- and two-qubit quantum gates. Meanwhile, Huang HL et al. (2021) devised a flexible QGAN to solve the task of generation of handwritten digit images with six superconducting qubits. Those experimental works provide guidance for the use of QGANs in near-term superconducting quantum processors. Further inspired by adversarial learning, Ren et al. (2022) first experimentally demonstrated a quantum adversarial learning algorithm on a 10-qubit superconducting chain for both real-life images and many-body quantum states.

6 Challenges and the future of digital quantum simulation

6.1 Limitations of superconducting qubits

Nevertheless, advanced superconducting transmon qubits still encounter several challenges. First, scaling up to large-scale superconducting quantum computers poses significant hurdles. The associated hardware necessitates an ultracold cryogenic environment and intricate microwave cabling, which collectively entail considerable spatial requirements. Merely expanding the physical footprint of a superconducting quantum computer, however, is not a prudent strategy to accomplish this. Moreover, the extensive connections of microwave wiring can induce unwanted thermal noise and intricate signal interference.

Noise within quantum circuits poses another challenge. This noise is primarily attributed to decoherence errors, a consequence of interactions with the environment, as well as leakage errors due to the limited anharmonicity of transmon qubits. Consequently, the implementation of effective QEC codes and strategies to mitigate leakage are imperative for the realization of fault-tolerant superconducting quantum computing. Addressing these issues is crucial for the progression and viability of superconducting-based quantum technology.

6.2 QEC for superconducting qubits

In the NISQ era, errors are inevitable during quantum logic operations due to imperfections in the physical hardware. In contrast to the case of classical computers, quantum information cannot be cloned, making error correction more complex. Here we discuss the surface code and Bosonic code for QEC based on superconducting qubits.

First, we consider the surface code (Bravyi and Kitaev, 1998; Freedman, 2001; Dennis et al., 2002), which is the planar version of the toric code (Kitaev, 2003). A notable advantage of surface code is its relatively high tolerance to local errors (Wang et al., 2003), due to the topological nature of the physical 2D system. In 2012, Fowler et al. (2012) introduced the stabilizer formed by two qubits for surface code quantum computing implemented in a 2D array of physical qubits, which aimed to perform parity measurements via the XXXX and ZZZZ stabilizer operators; accordingly, the errors occurring in the logical qubit could be determined. For probabilistic errors in superconducting

qubits, surface code is an efficient method for error correction (Barends et al., 2013; Kelly et al., 2015; Ataides et al., 2021; Krinner et al., 2022; Marques et al., 2022; Zhao et al., 2022; Google Quantum AI, 2023). Even though great progress has been achieved in the implementation of surface code with a relatively tolerant error threshold (Google Quantum AI, 2023), what is still formidable is the overhead of physical-to-logical qubits.

Bosonic code is another important branch of QEC with remarkable development (Cai et al., 2021; Ma et al., 2021). In such code, quantum information can be encoded into the infinite-dimensional subspace of a bosonic superconducting cavity mode. Cat code and binomial code are the two prototypical categories of bosonic code. The former demonstrates the suppression of the break-even point by promoting the error-corrected lifetime (Wang et al., 2016). The latter showcases the high-fidelity operations on a single logical qubit. On the other hand, Bosonic-encoded qubits can also build two-qubit gates, such as CNOT gates and SWAP-like gates, to generate entanglement states; this may pave the way for multiqubit fault-tolerant protocols.

Recently, both the implementation of surface code (Google Quantum AI, 2023) and Bosonic code (Ni et al., 2023; Sivak et al., 2023) have reached break-even points in a logical qubit, with the former result indicating that the error correction performance based on a larger-scale system is better. These breakthroughs have undoubtedly pushed large-scale QEC research forward. Newly, Google Quantum AI and collaborators implemented a distance-7 surface code with 101 superconducting qubits (Acharya et al., 2024), which further reduces the logic error rate below the critical threshold. We should be aware that superconducting quantum computing will likely stay in the NISQ era for a long time, until the development of optimal solutions for QEC.

6.3 Challenges for digital quantum simulation

In NISQ devices, the total operation duration of an effective digital superconducting circuit usually approaches the coherence dephasing time of about 20 μs. This extremely limits the power of quantum simulation. The challenges for digital quantum simulation comprise two aspects: logic gates and decomposition algorithms.

As for the logic gates, they require speed and high fidelity. At present, the fast single-qubit gate takes about 10 ns with a fidelity above 0.999, and the two-qubit gate is about 20 ns (Arute et al., 2019) with a fidelity of about 0.994. However, these performances are still unable to help to achieve quantum advantage in more practical applications. Investigating the relationship between time duration and fidelity and finding a new mechanism of two-qubit gates will require significant further research.

In terms of the decomposition algorithm, we know it generally possesses a high number of logic gates, and thus the efficient compile algorithm has a smaller number of logic gates for high-precision outcomes. Due to the extensive resource requirements, the scalability of digital quantum circuits is also limited.

6.4 Future improvements

Here we highlight several potential directions for digital quantum simulation based on superconducting quantum circuits.

6.4.1 Optimal performance of superconducting qubits

The coherence time of transmon qubits is at the scale of 100 μs (Google Quantum AI, 2023; Kim et al., 2023; Xu et al., 2023), which is still short compared to other platforms, and far beyond the requirement for deep quantum circuits. The simultaneous operation fidelity of single-qubit gates can surpass 0.999 (Google Quantum AI, 2023), while two-qubit gates are merely around 0.995 (Wu et al., 2021; Google Quantum AI, 2023; Xu et al., 2023). Thus, continuing to reduce the error rates of single-qubit gates and two-qubit gates requires increasingly more effort. Under the premise of long coherence time and high-fidelity logic gates, it is relevant to push for intermediate-to-large-scale superconducting quantum processors.

6.4.2 QEC and error mitigation

QEC is crucial for large-scale quantum devices, which can effectively protect logic operations from local errors. However, the resources for realizing fault tolerance with the aid of QEC require more than hundreds of thousands of qubits. Therefore, developing more quantum resource-efficient QEC is of vital importance. For the measurement error, this can be mitigated by developing efficient quantum error mitigation (QEM) algorithms (Cai et al., 2023).

6.4.3 Hybrid digital-analog quantum simulation

The alliance of digital and analog quantum simulation (Lamata et al., 2018) effectively integrates digital quantum gates and analog unitary blocks, leveraging the scalability of analog blocks and the flexibility of digital steps. Nowadays, digital-analog quantum simulation (DAQS) is considered a promising candidate for achieving quantum advantage with no requirement of QEC (Lamata et al., 2018; Parra-Rodriguez et al., 2020). In superconducting circuits, digital-analog quantum simulation has shed light onto many-body physics problems (Gong et al., 2023; Andersen et al., 2024). Nevertheless, there are numerous open problems in the way of establishing a formal paradigm of DAQS, such as the universality of DQAS, and the decomposition algorithm within the DAQS framework.

7 Conclusions

This review focused on digital quantum simulation applications implemented by superconducting quantum circuits. For quantum chemistry, the developed VQE with various ansatz contributes to the ground-state estimation of molecules, from simple H_2 to complex F_2, under the precision of chemistry accuracy. In terms of emerging quantum matters which are unfeasible in natural condensed-matter materials, the high-precision digital strategy provides a way to generate and manipulate these unique quantum matters, such as DTCs and non-Abelian anyons. In the emerging setting of quantum combinatorial optimization and quantum machine learning, many proof-of-concept applications have been developed. These reveal the impressive ability of digital quantum circuits to simulate chemical interactions and materials. Nevertheless, these applications are still achievable with classical computers.

We must be aware that superconducting digital quantum simulation still faces significant hurdles, as does superconducting quantum computing. Among them, unavoidable noise errors can significantly limit the duration of quantum logical operations. Therefore, it is important to promote the resource-efficient QEC and QEM, to enable more practical implementations aided by digital quantum simulation. By tackling the challenges of digital quantum simulation and superconducting qubits, superconducting digital quantum simulation may help build an anticipated future, describing more complex and exotic quantum matters, simulating molecules, and even leading to quantum optimization algorithms.

Acknowledgments

This work is supported by the National Natural Science Foundation of China (No. 12304559) and the Zhejiang Provincial Natural Science Foundation of China (No. LDQ23A040001).

Author contributions

Zhen WANG designed the research. Yunyan YAO and Zhen WANG processed the corresponding data. Yunyan YAO wrote the first draft of the manuscript. Yunyan YAO and Zhen WANG revised and edited the final version.

Conflict of interest

Yunyan YAO and Zhen WANG declare that they have no conflict of interest.

References

Abrams DM, Didier N, Johnson BR, et al., 2020. Implementation of XY entangling gates with a single calibrated pulse. *Nature Electronics*, 3(12):744-750. https://doi.org/10.1038/s41928-020-00498-1

Acharya R, Aghababaie-Beni L, Aleiner I, et al., 2024. Quantum error correction below the surface code threshold. arXiv:2408.13687. https://doi.org/10.48550/arXiv.2408.13687

Anand A, Schleich P, Alperin-Lea S, et al., 2022. A quantum computing view on unitary coupled cluster theory. *Chemical Society Reviews*, 51(5):1659-1684. https://doi.org/10.1039/D1CS00932J

Andersen TI, Astrakhantsev N, Karamlou AH, et al., 2024. Thermalization and criticality on an analog-digital quantum simulator. arXiv:2405.17385. https://doi.org/10.48550/arXiv.2405.17385

Arovas DP, Berg E, Kivelson SA, et al., 2022. The Hubbard model. *Annual Review of Condensed Matter Physics*, 13: 239-274. https://doi.org/10.1146/annurev-conmatphys-031620-102024

Arute F, Arya K, Babbush R, et al., 2019. Quantum supremacy using a programmable superconducting processor. *Nature*, 574(7779):505-510. https://doi.org/10.1038/s41586-019-1666-5

Aspuru-Guzik A, Dutoi AD, Love PJ, et al., 2005. Simulated quantum computation of molecular energies. *Science*, 309(5741):1704-1707. https://doi.org/10.1126/science.1113479

Aspuru-Guzik A, Walther P, 2012. Photonic quantum simulators. *Nature Physics*, 8(4):285-291. https://doi.org/10.1038/nphys2253

Ataides JPB, Tuckett DK, Bartlett SD, et al., 2021. The XZZX surface code. *Nature Communications*, 12(1):2172. https://doi.org/10.1038/s41467-021-22274-1

Azses D, Haenel R, Naveh Y, et al., 2020. Identification of symmetry-protected topological states on noisy quantum computers. *Physical Review Letters*, 125(12):120502. https://doi.org/10.1103/PhysRevLett.125.120502

Bao ZH, Xu SB, Song ZX, et al., 2024. Schrödinger cats growing up to 60 qubits and dancing in a cat scar enforced discrete time crystal. arXiv:2401.08284. https://doi.org/10.48550/arXiv.2401.08284

Barends R, Kelly J, Megrant A, et al., 2013. Coherent Josephson qubit suitable for scalable quantum integrated circuits. *Physical Review Letters*, 111(8):080502. https://doi.org/10.1103/PhysRevLett.111.080502

Barends R, Lamata L, Kelly J, et al., 2015. Digital quantum simulation of fermionic models with a superconducting circuit. *Nature Communications*, 6(1):7654. https://doi.org/10.1038/ncomms8654

Bartlett RJ, Kucharski SA, Noga J, 1989. Alternative coupled-cluster ansätze II. The unitary coupled-cluster method. *Chemical Physics Letters*, 155(1):133-140. https://doi.org/10.1016/S0009-2614(89)87372-5

Bauer CW, Davoudi Z, Balantekin AB, et al., 2023. Quantum simulation for high-energy physics. *PRX Quantum*, 4(2):027001. https://doi.org/10.1103/PRXQuantum.4.027001

Bengtsson A, Vikstål P, Warren C, et al., 2020. Improved success probability with greater circuit depth for the quantum approximate optimization algorithm. *Physical Review Applied*, 14(3):034010. https://doi.org/10.1103/PhysRevApplied.14.034010

Bharti K, Cervera-Lierta A, Kyaw TH, et al., 2022. Noisy intermediate-scale quantum algorithms. *Reviews of Modern Physics*, 94(1):015004. https://doi.org/10.1103/RevModPhys.94.015004

Biamonte J, Wittek P, Pancotti N, et al., 2017. Quantum machine learning. *Nature*, 549(7671):195-202. https://doi.org/10.1038/nature23474

Blais A, Huang RS, Wallraff A, et al., 2004. Cavity quantum electrodynamics for superconducting electrical circuits: an architecture for quantum computation. *Physical Review A*, 69(6):062320. https://doi.org/10.1103/PhysRevA.69.062320

Blatt R, Roos CF, 2012. Quantum simulations with trapped ions. *Nature Physics*, 8(4):277-284. https://doi.org/10.1038/nphys2252

Bluvstein D, Omran A, Levine H, et al., 2021. Controlling quantum many-body dynamics in driven Rydberg atom arrays. *Science*, 371(6536):1355-1359. https://doi.org/10.1126/science.abg2530

Bluvstein D, Evered SJ, Geim AA, et al., 2024. Logical quantum processor based on reconfigurable atom arrays. *Nature*, 626(7997):58-65. https://doi.org/10.1038/s41586-023-06927-3

Bravyi SB, Kitaev AY, 1998. Quantum codes on a lattice with boundary. arXiv:quant-ph/9811052. https://doi.org/10.48550/arXiv.quant-ph/9811052

Browaeys A, Lahaye T, 2020. Many-body physics with individually controlled rydberg atoms. *Nature Physics*, 16(2):132-142. https://doi.org/10.1038/s41567-019-0733-z

Cai WZ, Ma YW, Wang WT, et al., 2021. Bosonic quantum error correction codes in superconducting quantum circuits. *Fundamental Research*, 1(1):50-67. https://doi.org/10.1016/j.fmre.2020.12.006

Cai ZY, Babbush R, Benjamin SC, et al., 2023. Quantum error mitigation. *Reviews of Modern Physics*, 95(4):045005. https://doi.org/10.1103/RevModPhys.95.045005

Chai YH, Han YJ, Wu YC, et al., 2022. Shortcuts to the quantum approximate optimization algorithm. *Physical Review A*, 105(4):042415. https://doi.org/10.1103/PhysRevA.105.042415

Chen IC, Burdick B, Yao YX, et al., 2022. Error-mitigated simulation of quantum many-body scars on quantum computers with pulse-level control. *Physical Review Research*, 4(4):043027. https://doi.org/10.1103/PhysRevResearch.4.043027

Choo K, von Keyserlingk CW, Regnault N, et al., 2018. Measurement of the entanglement spectrum of a symmetry-protected topological state using the IBM quantum computer. *Physical Review Letters*, 121(8):086808. https://doi.org/10.1103/PhysRevLett.121.086808

Cirac JI, Zoller P, 2012. Goals and opportunities in quantum simulation. *Nature Physics*, 8(4):264-266. https://doi.org/10.1038/nphys2275

Clarke J, Wilhelm FK, 2008. Superconducting quantum bits. *Nature*, 453(7198):1031-1042. https://doi.org/10.1038/nature07128

Clarke J, Cleland AN, Devoret MH, et al., 1988. Quantum mechanics of a macroscopic variable: the phase difference of a josephson junction. *Science*, 239(4843):992-997. https://doi.org/10.1126/science.239.4843.992

Colless JI, Ramasesh VV, Dahlen D, et al., 2018. Computation of molecular spectra on a quantum processor with an error-resilient algorithm. *Physical Review X*, 8(1):011021. https://doi.org/10.1103/PhysRevX.8.011021

Cong I, Choi S, Lukin MD, 2019. Quantum convolutional neural networks. *Nature Physics*, 15(12):1273-1278. https://doi.org/10.1038/s41567-019-0648-8

Daley AJ, Bloch I, Kokail C, et al., 2022. Practical quantum advantage in quantum simulation. *Nature*, 607(7920):667-676. https://doi.org/10.1038/s41586-022-04940-6

Dallaire-Demers PL, Killoran N, 2018. Quantum generative adversarial networks. *Physical Review A*, 98(1):012324. https://doi.org/10.1103/PhysRevA.98.012324

Deng YH, Gong SQ, Gu YC, et al., 2023. Solving graph problems using Gaussian boson sampling. *Physical Review Letters*, 130(19):190601. https://doi.org/10.1103/PhysRevLett.130.190601

Dennis E, Kitaev A, Landahl A, et al., 2002. Topological quantum memory. *Journal of Mathematical Physics*, 43(9):4452-4505. https://doi.org/10.1063/1.1499754

Ding L, Hays M, Sung Y, et al., 2023. High-fidelity, frequency-flexible two-qubit fluxonium gates with a transmon coupler.

Physical Review X, 13(3):031035. https://doi.org/10.1103/PhysRevX.13.031035

DiVincenzo DP, 2000. The physical implementation of quantum computation. *Fortschritte der Physik*, 48(9-11):771-783. https://doi.org/10.1002/1521-3978(200009)48:9/11<771::AID-PROP771>3.0.CO;2-E

Dunjko V, Briegel HJ, 2018. Machine learning & artificial intelligence in the quantum domain: a review of recent progress. *Reports on Progress in Physics*, 81(7):074001. https://doi.org/10.1088/1361-6633/aab406

Eisert J, Friesdorf M, Gogolin C, 2015. Quantum many-body systems out of equilibrium. *Nature Physics*, 11(2):124-130. https://doi.org/10.1038/nphys3215

Else DV, Bauer B, Nayak C, 2016. Floquet time crystals. *Physical Review Letters*, 117(9):090402. https://doi.org/10.1103/PhysRevLett.117.090402

Else DV, Bauer B, Nayak C, 2017. Prethermal phases of matter protected by time-translation symmetry. *Physical Review X*, 7(1):011026. https://doi.org/10.1103/PhysRevX.7.011026

Else DV, Monroe C, Nayak C, et al., 2020. Discrete time crystals. *Annual Review of Condensed Matter Physics*, 11:467-499. https://doi.org/10.1146/annurev-conmatphys-031119-050658

Farhi E, Goldstone J, Gutmann S, 2014. A quantum approximate optimization algorithm. arXiv:1411.4028. https://doi.org/10.48550/arXiv.1411.4028

Feynman RP, 1982. Simulating physics with computers. *International Journal of Theoretical Physics*, 21(6):467-488. https://doi.org/10.1007/BF02650179

Foulkes WMC, Mitas L, Needs RJ, et al., 2001. Quantum Monte Carlo simulations of solids. *Reviews of Modern Physics*, 73(1):33-83. https://doi.org/10.1103/RevModPhys.73.33

Fowler AG, Mariantoni M, Martinis JM, et al., 2012. Surface codes: towards practical large-scale quantum computation. *Physical Review A*, 86(3):032324. https://doi.org/10.1103/PhysRevA.86.032324

Foxen B, Neill C, Dunsworth A, et al., 2020. Demonstrating a continuous set of two-qubit gates for near-term quantum algorithms. *Physical Review Letters*, 125(12):120504. https://doi.org/10.1103/PhysRevLett.125.120504

Freedman MH, 2001. Quantum computation and the localization of modular functors. *Foundations of Computational Mathematics*, 1(2):183-204. https://doi.org/10.1007/s102080010006

Frey P, Rachel S, 2022. Realization of a discrete time crystal on 57 qubits of a quantum computer. *Science Advances*, 8(9):eabm7652. https://doi.org/10.1126/sciadv.abm7652

Ganzhorn M, Egger DJ, Barkoutsos P, et al., 2019. Gate-efficient simulation of molecular eigenstates on a quantum computer. *Physical Review Applied*, 11(4):044092. https://doi.org/10.1103/PhysRevApplied.11.044092

Georgescu IM, Ashhab S, Nori F, 2014. Quantum simulation. *Reviews of Modern Physics*, 86(1):153-185. https://doi.org/10.1103/RevModPhys.86.153

Gong M, Huang HL, Wang SY, et al., 2023. Quantum neuronal sensing of quantum many-body states on a 61-qubit programmable superconducting processor. *Science Bulletin*, 68(9):906-912. https://doi.org/10.1016/j.scib.2023.04.003

Goodfellow IJ, Pouget-Abadie J, Mirza M, et al., 2014. Generative adversarial networks. arXiv:1406.2661. https://doi.org/10.48550/arXiv.1406.2661

Google AI Quantum and Collaborators, Arute F, Arya K, et al., 2020. Hartree-Fock on a superconducting qubit quantum computer. *Science*, 369(6507):1084-1089. https://doi.org/10.1126/science.abb9811

Google Quantum AI, 2023. Suppressing quantum errors by scaling a surface code logical qubit. *Nature*, 614(7949):676-681. https://doi.org/10.1038/s41586-022-05434-1

Google Quantum AI and Collaborators, 2023. Non-Abelian braiding of graph vertices in a superconducting processor. *Nature*, 618(7964):264-269. https://doi.org/10.1038/s41586-023-05954-4

Greiner M, Mandel O, Esslinger T, et al., 2002. Quantum phase transition from a superfluid to a Mott insulator in a gas of ultracold atoms. *Nature*, 415(6867):39-44. https://doi.org/10.1038/415039a

Guo SA, Wu YK, Ye J, et al., 2024. A site-resolved two-dimensional quantum simulator with hundreds of trapped ions. *Nature*, 630(8017):613-618. https://doi.org/10.1038/s41586-024-07459-0

Guo SJ, Sun JZ, Qian HR, et al., 2024. Experimental quantum computational chemistry with optimized unitary coupled cluster ansatz. *Nature Physics*, 20(8):1240-1246. https://doi.org/10.1038/s41567-024-02530-z

Haldar A, Sen D, Moessner R, et al., 2021. Dynamical freezing and scar points in strongly driven Floquet matter: resonance vs emergent conservation laws. *Physical Review X*, 11(2):021008. https://doi.org/10.1103/PhysRevX.11.021008

Harrigan MP, Sung KJ, Neeley M, et al., 2021. Quantum approximate optimization of non-planar graph problems on a planar superconducting processor. *Nature Physics*, 17(3):332-336. https://doi.org/10.1038/s41567-020-01105-y

Havlíček V, Córcoles AD, Temme K, et al., 2019. Supervised learning with quantum-enhanced feature spaces. *Nature*, 567(7747):209-212. https://doi.org/10.1038/s41586-019-0980-2

Henderson M, Shakya S, Pradhan S, et al., 2020. Quanvolutional neural networks: powering image recognition with quantum circuits. *Quantum Machine Intelligence*, 2(1):2. https://doi.org/10.1007/s42484-020-00012-y

Herrmann J, Llima SM, Remm A, et al., 2022. Realizing quantum convolutional neural networks on a superconducting quantum processor to recognize quantum phases. *Nature Communications*, 13(1):4144. https://doi.org/10.1038/s41467-022-31679-5

Heya K, Nakanishi KM, Mitarai K, et al., 2023. Subspace variational quantum simulator. *Physical Review Research*,

5(2):023078.
https://doi.org/10.1103/PhysRevResearch.5.023078

Hu L, Wu SH, Cai WZ, et al., 2019. Quantum generative adversarial learning in a superconducting quantum circuit. *Science Advances*, 5(1):eaav2761.
https://doi.org/10.1126/sciadv.aav2761

Huang B, 2023. Analytical theory of cat scars with discrete time-crystalline dynamics in Floquet systems. *Physical Review B*, 108(10):104309.
https://doi.org/10.1103/PhysRevB.108.104309

Huang HL, Du YX, Gong M, et al., 2021. Experimental quantum generative adversarial networks for image generation. *Physical Review Applied*, 16(2):024051.
https://doi.org/10.1103/PhysRevApplied.16.024051

Huang KX, Wang ZA, Song C, et al., 2021. Quantum generative adversarial networks with multiple superconducting qubits. *npj Quantum Information*, 7(1):165.
https://doi.org/10.1038/s41534-021-00503-1

Huang KX, Cai XX, Li H, et al., 2022. Variational quantum computation of molecular linear response properties on a superconducting quantum processor. *The Journal of Physical Chemistry Letters*, 13(39):9114-9121.
https://doi.org/10.1021/acs.jpclett.2c02381

Huggins WJ, O'Gorman BA, Rubin NC, et al., 2022. Unbiasing fermionic quantum Monte Carlo with a quantum computer. *Nature*, 603(7901):416-420.
https://doi.org/10.1038/s41586-021-04351-z

Ippoliti M, Kechedzhi K, Moessner R, et al., 2021. Many-body physics in the NISQ era: quantum programming a discrete time crystal. *PRX Quantum*, 2(3):030346.
https://doi.org/10.1103/PRXQuantum.2.030346

Jerbi S, Fiderer LJ, Nautrup HP, et al., 2023. Quantum machine learning beyond kernel methods. *Nature Communications*, 14(1):517.
https://doi.org/10.1038/s41467-023-36159-y

Jin YX, Xu HZ, Wang ZA, et al., 2024. Quafu-RL: the cloud quantum computers based quantum reinforcement learning. *Chinese Physics B*, 33(5):050301.
https://doi.org/10.1088/1674-1056/ad3061

Kandala A, Mezzacapo A, Temme K, et al., 2017. Hardware-efficient variational quantum eigensolver for small molecules and quantum magnets. *Nature*, 549(7671):242-246.
https://doi.org/10.1038/nature23879

Kandala A, Temme K, Córcoles AD, et al., 2019. Error mitigation extends the computational reach of a noisy quantum processor. *Nature*, 567(7749):491-495.
https://doi.org/10.1038/s41586-019-1040-7

Karamlou AH, Simon WA, Katabarwa A, et al., 2021. Analyzing the performance of variational quantum factoring on a superconducting quantum processor. *npj Quantum Information*, 7(1):156.
https://doi.org/10.1038/s41534-021-00478-z

Kelly J, Barends R, Fowler AG, et al., 2015. State preservation by repetitive error detection in a superconducting quantum circuit. *Nature*, 519(7541):66-69.
https://doi.org/10.1038/nature14270

Kerenidis I, Landman J, Prakash A, 2020. Quantum algorithms for deep convolutional neural networks. Proceedings of the 8th International Conference on Learning Representations.

Killoran N, Lee LJ, Delong A, et al., 2017. Generating and designing DNA with deep generative models. arXiv:1712.06148.
https://doi.org/10.48550/arXiv.1712.06148

Kim Y, Eddins A, Anand S, et al., 2023. Evidence for the utility of quantum computing before fault tolerance. *Nature*, 618(7965):500-505.
https://doi.org/10.1038/s41586-023-06096-3

Kirmani A, Bull K, Hou CY, et al., 2022. Probing geometric excitations of fractional quantum hall states on quantum computers. *Physical Review Letters*, 129(5):056801.
https://doi.org/10.1103/PhysRevLett.129.056801

Kitaev A, Preskill J, 2006. Topological entanglement entropy. *Physical Review Letters*, 96(11):110404.
https://doi.org/10.1103/PhysRevLett.96.110404

Kitaev AY, 1997. Quantum computations: algorithms and error correction. *Russian Mathematical Surveys*, 52(6):1191-1249.
https://doi.org/10.1070/RM1997v052n06ABEH002155

Kitaev AY, 2001. Unpaired Majorana fermions in quantum wires. *Physics-Uspekhi*, 44(10S):131-136.
https://doi.org/10.1070/1063-7869/44/10S/S29

Kitaev AY, 2003. Fault-tolerant quantum computation by anyons. *Annals of Physics*, 303(1):2-30.
https://doi.org/10.1016/S0003-4916(02)00018-0

Koch J, Yu TM, Gambetta J, et al., 2007. Charge-insensitive qubit design derived from the Cooper pair box. *Physical Review A*, 76(4):042319.
https://doi.org/10.1103/PhysRevA.76.042319

Koh JM, Tai T, Lee CH, 2022a. Simulation of interaction-induced chiral topological dynamics on a digital quantum computer. *Physical Review Letters*, 129(14):140502.
https://doi.org/10.1103/PhysRevLett.129.140502

Koh JM, Tai T, Phee YH, et al., 2022b. Stabilizing multiple topological fermions on a quantum computer. *npj Quantum Information*, 8(1):16.
https://doi.org/10.1038/s41534-022-00527-1

Krantz P, Kjaergaard M, Yan F, et al., 2019. A quantum engineer's guide to superconducting qubits. *Applied Physics Reviews*, 6(2):021318.
https://doi.org/10.1063/1.5089550

Krinner S, Lacroix N, Remm A, et al., 2022. Realizing repeated quantum error correction in a distance-three surface code. *Nature*, 605(7911):669-674.
https://doi.org/10.1038/s41586-022-04566-8

Krizhevsky A, Sutskever I, Hinton GE, 2017. ImageNet classification with deep convolutional neural networks. *Communications of the ACM*, 60(6):84-90.
https://doi.org/10.1145/3065386

Kyprianidis A, Machado F, Morong W, et al., 2021. Observation of a prethermal discrete time crystal. *Science*, 372(6547):1192-1196.
https://doi.org/10.1126/science.abg8102

Lamata L, Parra-Rodriguez A, Sanz M, et al., 2018. Digital-analog quantum simulations with superconducting circuits. *Advances in Physics: X*, 3(1):1457981.
https://doi.org/10.1080/23746149.2018.1457981

Lanyon BP, Hempel C, Nigg D, et al., 2011. Universal digital quantum simulation with trapped ions. *Science*, 334(6052):

57-61.
https://doi.org/10.1126/science.1208001

Lecun Y, Bottou L, Bengio Y, et al., 1998. Gradient-based learning applied to document recognition. *Proceedings of the IEEE*, 86(11):2278-2324.
https://doi.org/10.1109/5.726791

LeCun Y, Bengio Y, Hinton G, 2015. Deep learning. *Nature*, 521(7553):436-444.
https://doi.org/10.1038/nature14539

Ledig C, Theis L, Huszár F, et al., 2017. Photo-realistic single image super-resolution using a generative adversarial network. IEEE Conference on Computer Vision and Pattern Recognition, p.105-114.
https://doi.org/10.1109/CVPR.2017.19

Levin M, Wen XG, 2006. Detecting topological order in a ground state wave function. *Physical Review Letters*, 96(11):110405.
https://doi.org/10.1103/PhysRevLett.96.110405

Li ZK, Liu XM, Xu NY, et al., 2015. Experimental realization of a quantum support vector machine. *Physical Review Letters*, 114(14):140504.
https://doi.org/10.1103/PhysRevLett.114.140504

Lian B, Sun XQ, Vaezi A, et al., 2018. Topological quantum computation based on chiral Majorana fermions. *Proceedings of the National Academy of Sciences of the United States of America*, 115(43):10938-10942.
https://doi.org/10.1073/pnas.1810003115

Liu JH, Lim KH, Wood KL, et al., 2021. Hybrid quantum-classical convolutional neural networks. *Science China Physics, Mechanics & Astronomy*, 64(9):290311.
https://doi.org/10.1007/s11433-021-1734-3

Lloyd S, 1996. Universal quantum simulators. *Science*, 273(5278):1073-1078.
https://doi.org/10.1126/science.273.5278.1073

Lloyd S, Weedbrook C, 2018. Quantum generative adversarial learning. *Physical Review Letters*, 121(4):040502.
https://doi.org/10.1103/PhysRevLett.121.040502

Loss D, DiVincenzo DP, 1998. Quantum computation with quantum dots. *Physical Review A*, 57(1):120-126.
https://doi.org/10.1103/PhysRevA.57.120

Ma WL, Puri S, Schoelkopf RJ, et al., 2021. Quantum control of bosonic modes with superconducting circuits. *Science Bulletin*, 66(17):1789-1805.
https://doi.org/10.1016/j.scib.2021.05.024

Machado F, Else DV, Kahanamoku-Meyer GD, et al., 2020. Long-range prethermal phases of nonequilibrium matter. *Physical Review X*, 10(1):011043.
https://doi.org/10.1103/PhysRevX.10.011043

Marques JF, Varbanov BM, Moreira MS, et al., 2022. Logical-qubit operations in an error-detecting surface code. *Nature Physics*, 18(1):80-86.
https://doi.org/10.1038/s41567-021-01423-9

Martinis JM, Nam S, Aumentado J, et al., 2002. Rabi oscillations in a large josephson-junction qubit. *Physical Review Letters*, 89(11):117901.
https://doi.org/10.1103/PhysRevLett.89.117901

Maskara N, Michailidis AA, Ho WW, et al., 2021. Discrete time-crystalline order enabled by quantum many-body scars: entanglement steering via periodic driving. *Physical Review Letters*, 127(9):090602.
https://doi.org/10.1103/PhysRevLett.127.090602

Mathieu M, Couprie C, LeCun Y, 2016. Deep multi-scale video prediction beyond mean square error. The 4th International Conference on Learning Representations.

McArdle S, Endo S, Aspuru-Guzik A, et al., 2020. Quantum computational chemistry. *Reviews of Modern Physics*, 92(1):015003.
https://doi.org/10.1103/RevModPhys.92.015003

McClean JR, Boixo S, Smelyanskiy VN, et al., 2018. Barren plateaus in quantum neural network training landscapes. *Nature Communications*, 9(1):4812.
https://doi.org/10.1038/s41467-018-07090-4

Mi X, Sonner M, Niu MY, et al., 2022a. Noise-resilient edge modes on a chain of superconducting qubits. *Science*, 378(6621):785-790.
https://doi.org/10.1126/science.abq5769

Mi X, Ippoliti M, Quintana C, et al., 2022b. Time-crystalline eigenstate order on a quantum processor. *Nature*, 601(7894):531-536.
https://doi.org/10.1038/s41586-021-04257-w

Mizuta K, Takasan K, Kawakami N, 2020. Exact Floquet quantum many-body scars under Rydberg blockade. *Physical Review Research*, 2(3):033284.
https://doi.org/10.1103/PhysRevResearch.2.033284

Motta M, Sun C, Tan ATK, et al., 2020. Determining eigenstates and thermal states on a quantum computer using quantum imaginary time evolution. *Nature Physics*, 16(2):205-210.
https://doi.org/10.1038/s41567-019-0704-4

Mukherjee B, Nandy S, Sen A, et al., 2020. Collapse and revival of quantum many-body scars via Floquet engineering. *Physical Review B*, 101(24):245107.
https://doi.org/10.1103/PhysRevB.101.245107

Nakamura Y, Pashkin YA, Tsai JS, 1999. Coherent control of macroscopic quantum states in a single-cooper-pair box. *Nature*, 398(6730):786-788.
https://doi.org/10.1038/19718

Neill C, Roushan P, Kechedzhi K, et al., 2018. A blueprint for demonstrating quantum supremacy with superconducting qubits. *Science*, 360(6385):195-199.
https://doi.org/10.1126/science.aao4309

Ni ZC, Li S, Deng XW, et al., 2023. Beating the break-even point with a discrete-variable-encoded logical qubit. *Nature*, 616(7955):56-60.
https://doi.org/10.1038/s41586-023-05784-4

O'Brien TE, Senjean B, Sagastizabal R, et al., 2019. Calculating energy derivatives for quantum chemistry on a quantum computer. *npj Quantum Information*, 5(1):113.
https://doi.org/10.1038/s41534-019-0213-4

O'Brien TE, Anselmetti G, Gkritsis F, et al., 2023. Purification-based quantum error mitigation of pair-correlated electron simulations. *Nature Physics*, 19(12):1787-1792.
https://doi.org/10.1038/s41567-023-02240-y

O'Malley P, Babbush R, Kivlichan I, et al., 2016. Scalable quantum simulation of molecular energies. *Physical Review X*, 6(3):031007.
https://doi.org/10.1103/PhysRevX.6.031007

Otterbach JS, Manenti R, Alidoust N, et al., 2017. Unsupervised machine learning on a hybrid quantum computer. arXiv:1712.05771.
https://doi.org/10.48550/arXiv.1712.05771

Parra-Rodriguez A, Lougovski P, Lamata L, et al., 2020. Digital-analog quantum computation. *Physical Review A*, 101(2):022305.
https://doi.org/10.1103/PhysRevA.101.022305

Pechal M, Roy F, Wilkinson SA, et al., 2022. Direct implementation of a perceptron in superconducting circuit quantum hardware. *Physical Review Research*, 4(3):033190.
https://doi.org/10.1103/PhysRevResearch.4.033190

Peters E, Caldeira J, Ho A, et al., 2021. Machine learning of high dimensional data on a noisy quantum processor. *npj Quantum Information*, 7(1):161.
https://doi.org/10.1038/s41534-021-00498-9

Place APM, Rodgers LVH, Mundada P, et al., 2021. New material platform for superconducting transmon qubits with coherence times exceeding 0.3 milliseconds. *Nature Communications*, 12(1):1779.
https://doi.org/10.1038/s41467-021-22030-5

Preskill J, 2012. Quantum computing and the entanglement frontier. arXiv:1203.5813.
https://doi.org/10.48550/arXiv.1203.5813

Preskill J, 2018. Quantum Computing in the NISQ era and beyond. *Quantum*, 2:79.
https://doi.org/10.22331/q-2018-08-06-79

Qin MP, Schäfer T, Andergassen S, et al., 2022. The hubbard model: a computational perspective. *Annual Review of Condensed Matter Physics*, 13:275-302.
https://doi.org/10.1146/annurev-conmatphys-090921-033948

Rahmani A, Sung KJ, Putterman H, et al., 2020. Creating and manipulating a laughlin-type ν=1/3 fractional quantum hall state on a quantum computer with linear depth circuits. *PRX Quantum*, 1(2):020309.
https://doi.org/10.1103/PRXQuantum.1.020309

Rebentrost P, Mohseni M, Lloyd S, 2014. Quantum support vector machine for big data classification. *Physical Review Letters*, 113(13):130503.
https://doi.org/10.1103/PhysRevLett.113.130503

Ren WH, Li WK, Xu SB, et al., 2022. Experimental quantum adversarial learning with programmable superconducting qubits. *Nature Computational Science*, 2(11):711-717.
https://doi.org/10.1038/s43588-022-00351-9

Reuer K, Landgraf J, Fösel T, et al., 2022. Realizing a deep reinforcement learning agent discovering real-time feedback control strategies for a quantum system. arXiv:2210.16715.
https://doi.org/10.48550/arXiv.2210.16715

Ristè D, da Silva MP, Ryan CA, et al., 2017. Demonstration of quantum advantage in machine learning. *npj Quantum Information*, 3(1):16.
https://doi.org/10.1038/s41534-017-0017-3

Romero J, Babbush R, McClean JR, et al., 2019. Strategies for quantum computing molecular energies using the unitary coupled cluster ansatz. *Quantum Science and Technology*, 4(1):014008.
https://doi.org/10.1088/2058-9565/aad3e4

Rosenberg E, Andersen TI, Samajdar R, et al., 2024. Dynamics of magnetization at infinite temperature in a Heisenberg spin chain. *Science*, 384(6691):48-53.
https://doi.org/10.1126/science.adi7877

Roushan P, Neill C, Chen Y, et al., 2014. Observation of topological transitions in interacting quantum circuits. *Nature*, 515(7526):241-244.
https://doi.org/10.1038/nature13891

Sagastizabal R, Bonet-Monroig X, Singh M, et al., 2019. Experimental error mitigation via symmetry verification in a variational quantum eigensolver. *Physical Review A*, 100(1):010302.
https://doi.org/10.1103/PhysRevA.100.010302

Salathé Y, Mondal M, Oppliger M, et al., 2015. Digital quantum simulation of spin models with circuit quantum electrodynamics. *Physical Review X*, 5(2):021027.
https://doi.org/10.1103/PhysRevX.5.021027

Salimans T, Goodfellow I, Zaremba W, et al., 2016. Improved techniques for training GANs. Proceedings of the 30th International Conference on Neural Information Processing Systems, p.2234-2242.

Sarma SD, Freedman M, Nayak C, 2015. Majorana zero modes and topological quantum computation. *npj Quantum Information*, 1(1):15001.
https://doi.org/10.1038/npjqi.2015.1

Satzinger KJ, Liu YJ, Smith A, et al., 2021. Realizing topologically ordered states on a quantum processor. *Science*, 374(6572):1237-1241.
https://doi.org/10.1126/science.abi8378

Schroer MD, Kolodrubetz MH, Kindel WF, et al., 2014. Measuring a topological transition in an artificial spin-1/2 system. *Physical Review Letters*, 113(5):050402.
https://doi.org/10.1103/PhysRevLett.113.050402

Schuld M, 2021. Supervised quantum machine learning models are kernel methods. arXiv:2101.11020.
https://doi.org/10.48550/arXiv.2101.11020

Schuld M, Killoran N, 2019. Quantum machine learning in feature hilbert spaces. *Physical Review Letters*, 122(4):040504.
https://doi.org/10.1103/PhysRevLett.122.040504

Schuld M, Sinayskiy I, Petruccione F, 2015. An introduction to quantum machine learning. *Contemporary Physics*, 56(2):172-185.
https://doi.org/10.1080/00107514.2014.964942

Schuster DI, Wallraff A, Blais A, et al., 2005. ac Stark shift and dephasing of a superconducting qubit strongly coupled to a cavity field. *Physical Review Letters*, 94(12):123602.
https://doi.org/10.1103/PhysRevLett.94.123602

Serbyn M, Abanin DA, Papić Z, 2021. Quantum many-body scars and weak breaking of ergodicity. *Nature Physics*, 17(6):675-685.
https://doi.org/10.1038/s41567-021-01230-2

Sherrington D, Kirkpatrick S, 1975. Solvable model of a spin-glass. *Physical Review Letters*, 35(26):1792-1796.
https://doi.org/10.1103/PhysRevLett.35.1792

Sivak VV, Eickbusch A, Royer B, et al., 2023. Real-time quantum error correction beyond break-even. *Nature*, 616(7955):

50-55.
https://doi.org/10.1038/s41586-023-05782-6

Smith A, Jobst B, Green AG, et al., 2022. Crossing a topological phase transition with a quantum computer. *Physical Review Research*, 4(2):L022020.
https://doi.org/10.1103/PhysRevResearch.4.L022020

Stern A, Lindner NH, 2013. Topological quantum computation—from basic concepts to first experiments. *Science*, 339(6124):1179-1184.
https://doi.org/10.1126/science.1231473

Streif M, Leib M, 2019. Comparison of QAOA with quantum and simulated annealing. arXiv:1901.01903.
https://doi.org/10.48550/arXiv.1901.01903

Sung Y, Ding L, Braumüller J, et al., 2021. Realization of high-fidelity CZ and *ZZ*-free iSWAP gates with a tunable coupler. *Physical Review X*, 11(2):021058.
https://doi.org/10.1103/PhysRevX.11.021058

Suzuki M, 1976. Generalized Trotter's formula and systematic approximants of exponential operators and inner derivations with applications to many-body problems. *Communications in Mathematical Physics*, 51(2):183-190.
https://doi.org/10.1007/BF01609348

Tan XS, Zhao YX, Liu Q, et al., 2017. Realizing and manipulating space-time inversion symmetric topological semimetal bands with superconducting quantum circuits. *npj Quantum Materials*, 2(1):60.
https://doi.org/10.1038/s41535-017-0062-3

Tan XS, Zhang DW, Liu Q, et al., 2018. Topological Maxwell metal bands in a superconducting qutrit. *Physical Review Letters*, 120(3):130503.
https://doi.org/10.1103/PhysRevLett.120.130503

Tan XS, Zhao YX, Liu Q, et al., 2019. Simulation and manipulation of tunable Weyl-semimetal bands using superconducting quantum circuits. *Physical Review Letters*, 122(1):010501.
https://doi.org/10.1103/PhysRevLett.122.010501

Tazhigulov RN, Sun SN, Haghshenas R, et al., 2022. Simulating models of challenging correlated molecules and materials on the Sycamore quantum processor. *PRX Quantum*, 3(4):040318.
https://doi.org/10.1103/PRXQuantum.3.040318

Trotter HF, 1959. On the product of semi-groups of operators. *Proceedings of the American Mathematical Society*, 10(4):545-551.
https://doi.org/10.1090/S0002-9939-1959-0108732-6

Turner CJ, Michailidis AA, Abanin DA, et al., 2018. Weak ergodicity breaking from quantum many-body scars. *Nature Physics*, 14(7):745-749.
https://doi.org/10.1038/s41567-018-0137-5

Viyuela O, Rivas A, Gasparinetti S, et al., 2018. Observation of topological Uhlmann phases with superconducting qubits. *npj Quantum Information*, 4(1):10.
https://doi.org/10.1038/s41534-017-0056-9

Wang C, Gao YY, Reinhold P, et al., 2016. A Schrödinger cat living in two boxes. *Science*, 352(6289):1087-1091.
https://doi.org/10.1126/science.aaf2941

Wang CL, Li XG, Xu HK, et al., 2022. Towards practical quantum computers: transmon qubit with a lifetime approaching 0.5 milliseconds. *npj Quantum Information*, 8(1):3.
https://doi.org/10.1038/s41534-021-00510-2

Wang CY, Harrington J, Preskill J, 2003. Confinement-Higgs transition in a disordered gauge theory and the accuracy threshold for quantum memory. *Annals of Physics*, 303(1):31-58.
https://doi.org/10.1016/S0003-4916(02)00019-2

Wang S, Fontana E, Cerezo M, et al., 2021. Noise-induced barren plateaus in variational quantum algorithms. *Nature Communications*, 12(1):6961.
https://doi.org/10.1038/s41467-021-27045-6

Wang ZT, Chen QH, Du YX, et al., 2024. Quantum compiling with reinforcement learning on a superconducting processor. arXiv:2406.12195.
https://doi.org/10.48550/arXiv.2406.12195

Weber JR, Koehl WF, Varley JB, et al., 2010. Quantum computing with defects. *Proceedings of the National Academy of Sciences of the United States of America*, 107(19):8513-8518.
https://doi.org/10.1073/pnas.1003052107

Wei SJ, Chen YH, Zhou ZR, et al., 2022. A quantum convolutional neural network on NISQ devices. *AAPPS Bulletin*, 32(1):2.
https://doi.org/10.1007/s43673-021-00030-3

Wen XG, 2017. Colloquium: zoo of quantum-topological phases of matter. *Reviews of Modern Physics*, 89(4):041004.
https://doi.org/10.1103/RevModPhys.89.041004

Wu YL, Bao WS, Cao S, et al., 2021. Strong quantum computational advantage using a superconducting quantum processor. *Physical Review Letters*, 127(18):180501.
https://doi.org/10.1103/PhysRevLett.127.180501

Xiang ZC, Huang KX, Zhang YR, et al., 2023. Simulating Chern insulators on a superconducting quantum processor. *Nature Communications*, 14(1):5433.
https://doi.org/10.1038/s41467-023-41230-9

Xu HK, Zhang JN, Han JX, et al., 2021. Realizing discrete time crystal in an one-dimensional superconducting qubit chain. arXiv:2108.00942.
https://doi.org/10.48550/arXiv.2108.00942

Xu HZ, Zhuang WF, Wang ZA, et al., 2024. Quafu-Qcover: explore combinatorial optimization problems on cloud-based quantum computers. *Chinese Physics B*, 33(5):050302.
https://doi.org/10.1088/1674-1056/ad18ab

Xu K, Ning W, Huang XJ, et al., 2021. Demonstration of a non-Abelian geometric controlled-NOT gate in a superconducting circuit. *Optica*, 8(7):972-976.
https://doi.org/10.1364/OPTICA.416264

Xu SB, Sun ZZ, Wang K, et al., 2023. Digital simulation of projective non-Abelian anyons with 68 superconducting qubits. *Chinese Physics Letters*, 40(6):060301.
https://doi.org/10.1088/0256-307X/40/6/060301

Xu SB, Sun ZZ, Wang K, et al., 2024. Non-Abelian braiding of Fibonacci anyons with a superconducting processor. *Nature Physics*, 20(9):1469-1475.
https://doi.org/10.1038/s41567-024-02529-6

Yan F, Krantz P, Sung Y, et al., 2018. Tunable coupling scheme for implementing high-fidelity two-qubit gates. *Physical*

Review Applied, 10(5):054062. https://doi.org/10.1103/PhysRevApplied.10.054062

Yao YY, Xiang L, 2024. Superconducting quantum simulation for many-body physics beyond equilibrium. *Entropy*, 26(7):592. https://doi.org/10.3390/e26070592

Yarloo H, Kopaei AE, Langari A, 2020. Homogeneous Floquet time crystal from weak ergodicity breaking. *Physical Review B*, 102(22):224309. https://doi.org/10.1103/PhysRevB.102.224309

Ying C, Guo QH, Li SW, et al., 2022. Floquet prethermal phase protected by U(1) symmetry on a superconducting quantum processor. *Physical Review A*, 105(1):012418. https://doi.org/10.1103/PhysRevA.105.012418

Yu YL, Cao CF, Dewey C, et al., 2022. Quantum approximate optimization algorithm with adaptive bias fields. *Physical Review Research*, 4(2):023249. https://doi.org/10.1103/PhysRevResearch.4.023249

Yu YL, Cao CF, Wang XB, et al., 2023. Solution of SAT problems with the adaptive-bias quantum approximate optimization algorithm. *Physical Review Research*, 5(2):023147. https://doi.org/10.1103/PhysRevResearch.5.023147

Zhang J, Hess PW, Kyprianidis A, et al., 2017. Observation of a discrete time crystal. *Nature*, 543(7644):217-220. https://doi.org/10.1038/nature21413

Zhang X, Jiang WJ, Deng JF, et al., 2022. Digital quantum simulation of Floquet symmetry-protected topological phases. *Nature*, 607(7919):468-473. https://doi.org/10.1038/s41586-022-04854-3

Zhao YW, Ye YS, Huang HL, et al., 2022. Realization of an error-correcting surface code with superconducting qubits. *Physical Review Letters*, 129(3):030501. https://doi.org/10.1103/PhysRevLett.129.030501

Zhong HS, Wang H, Deng YH, et al., 2020. Quantum computational advantage using photons. *Science*, 370(6523):1460-1463. https://doi.org/10.1126/science.abe8770

Zhou L, Wang ST, Choi S, et al., 2020. Quantum approximate optimization algorithm: performance, mechanism, and implementation on near-term devices. *Physical Review X*, 10(2):021067. https://doi.org/10.1103/PhysRevX.10.021067

Zhu LH, Tang HL, Barron GS, et al., 2022. Adaptive quantum approximate optimization algorithm for solving combinatorial problems on a quantum computer. *Physical Review Research*, 4(3):033029. https://doi.org/10.1103/PhysRevResearch.4.033029

Zhu QL, Cao SR, Chen FS, et al., 2022. Quantum computational advantage via 60-qubit 24-cycle random circuit sampling. *Science Bulletin*, 67(3):240-245. https://doi.org/10.1016/j.scib.2021.10.017